

Contact mechanics and elements of tribology

Lecture 4.

Micromechanical contact: roughness

Vladislav A. Yastrebov

*MINES ParisTech, PSL University, Centre des Matériaux, CNRS UMR 7633, Evry,
France*

@ Centre des Matériaux
February 25, 2020

- Introduction
- Measurement techniques
- Classifications
- Main characteristics
- PDF and PSD
- Random process model of roughness
- Computational roughness models
- Reading

Roughness

- Natural and industrial surfaces are *rough*:

- processing
- polishing
- coating
- microstructure
- surface energy
- deformation
- aging
- environment

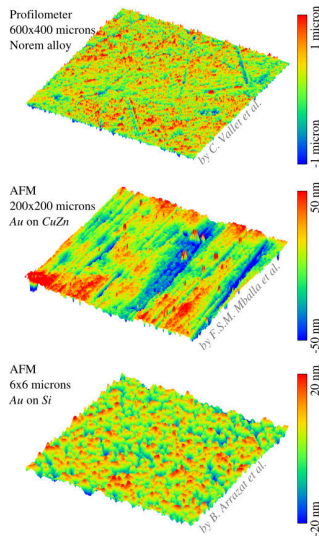


Fig. Examples of rough surfaces

Roughness

- Natural and industrial surfaces are *rough*:

- processing
- polishing
- coating
- microstructure
- surface energy
- deformation
- aging
- environment

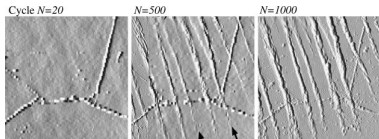


Fig. Persistent slip marks [1]

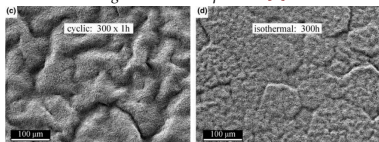


Fig. Rumpling (thermal cycling induced roughness in air)[2]

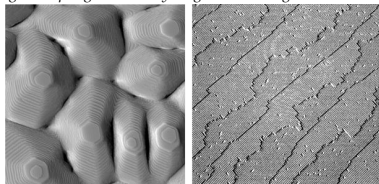


Fig. Epitaxial surface growth [3,4]

[1] J.Polák, J. Man & K. Orbtlík, Int J Fatigue 25 (2003)

[2] V.K. Tolpygo, D.R. Clarke, Acta Mat 52 (2004)

[3] M. Einax, W. Dieterich, P. Maass, Rev Mod Phys 85 (2013)
[4] H.B. Arlitt, G. S. C. 520 (2002)

Roughness

- Natural and industrial surfaces are *rough*:

- processing
- polishing
- coating
- microstructure
- surface energy
- deformation
- aging
- environment

- Roughness affects:

- stress-strain state
- dry friction
- wear
- adhesion
- fluid flow
- sealing
- energy transfer

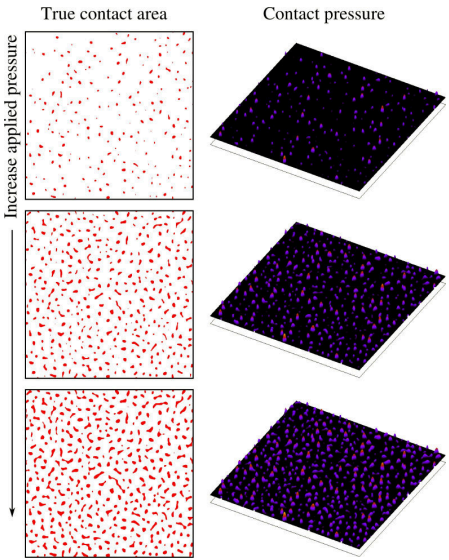


Fig. True contact area and stress fluctuations

Roughness

- Natural and industrial surfaces are *rough*:

- processing
- polishing
- coating
- microstructure
- surface energy
- deformation
- aging
- environment

- Roughness affects:

- stress-strain state
- dry friction
- wear
- adhesion
- fluid flow
- sealing
- energy transfer

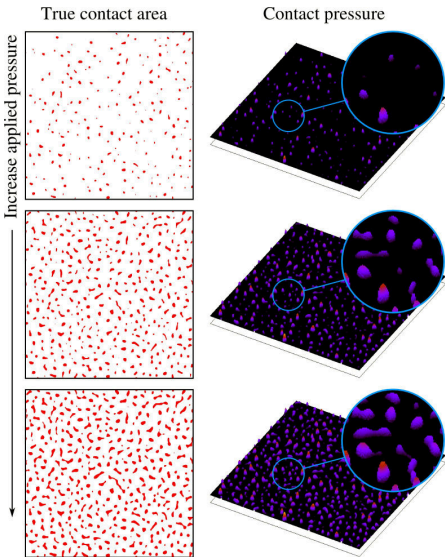


Fig. True contact area and stress fluctuations

Roughness

- Natural and industrial surfaces are *rough*:

- processing
- polishing
- coating
- microstructure
- surface energy
- deformation
- aging
- environment

- Roughness affects:

- stress-strain state
- dry friction
- wear
- adhesion
- fluid flow
- sealing
- energy transfer

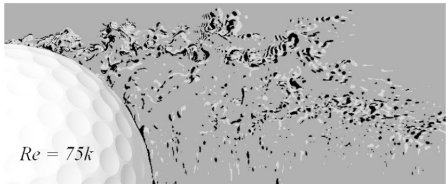
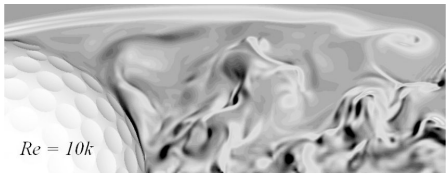


Fig. Numerical simulation of airflow around a (dimpled) golf ball [5]

Roughness

- Natural and industrial surfaces are *rough*:

- processing
- polishing
- coating
- microstructure
- surface energy
- deformation
- aging
- environment

- Roughness affects:

- stress-strain state
- dry friction
- wear
- adhesion
- fluid flow
- sealing
- energy transfer

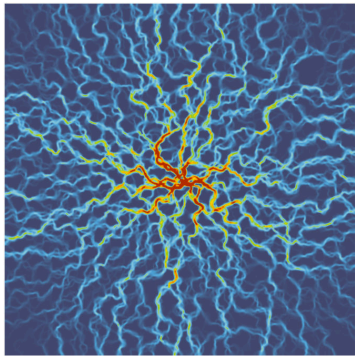


Fig. Fluid passage through free volume between rough surfaces

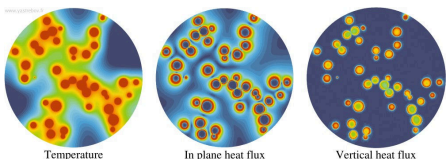


Fig. Heat transfer between rough surfaces
(asperity-based model)

Surface metrology techniques

■ Stylus measurements

- Mechanical contact of a tip with surface
- Force $\geq 3\mu\text{g}$, tip radius $\geq 50\text{ nm}$
- Mainly for profile measurements $y(x)$

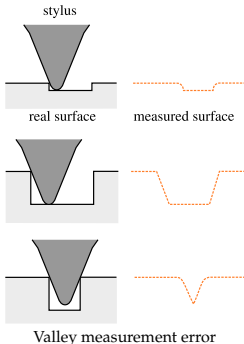
■ Optical measurements

- Confocal (laser scanning) microscopy
- *highest lateral resolution*
- Interferometry (WLI):
- *highest vertical resolution*
- *10 to 100 times faster than CM*
- Scanning Electronic Microscopy (SEM):
- *in secondary electron emission*
- *electrons penetrate in the matter → roughness smoothing*
- *conducting materials*

■ Nano-contact measurements

- Atomic Force Microscopy (AFM)
roughness + adhesive and elastic properties
- Scanning Tunneling Microscope (STM)

Stylus profilometer



Valley measurement error

Surface metrology techniques

■ Stylus measurements

- Mechanical contact of a tip with surface
- Force $\geq 3\mu\text{g}$, tip radius $\geq 50\text{ nm}$
- Mainly for profile measurements $y(x)$

■ Optical measurements

- Confocal (laser scanning) microscopy
 - *highest lateral resolution*
- Interferometry (WLI):
 - *highest vertical resolution*
 - *10 to 100 times faster than CM*
- Scanning Electronic Microscopy (SEM):
 - *in secondary electron emission*
 - *electrons penetrate in the matter → roughness smoothing*
 - *conducting materials*

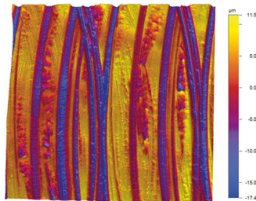
■ Nano-contact measurements

- Atomic Force Microscopy (AFM)
roughness + adhesive and elastic properties
- Scanning Tunneling Microscope (STM)

Stylus profilometer



Modern stylus profilometer
www.bruker.com



Roughness measurements ($\Delta z \approx 30\text{ }\mu\text{m}$)
www.icryst.com

Surface metrology techniques

■ Stylus measurements

- Mechanical contact of a tip with surface
- Force $\geq 3\mu\text{g}$, tip radius $\geq 50\text{ nm}$
- Mainly for profile measurements $y(x)$

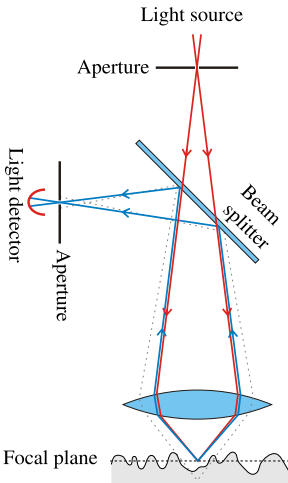
■ Optical measurements

- Confocal (laser scanning) microscopy
 - *highest lateral resolution*
- Interferometry (WLI):
 - *highest vertical resolution*
 - *10 to 100 times faster than CM*
- Scanning Electronic Microscopy (SEM):
 - *in secondary electron emission*
 - *electrons penetrate in the matter → roughness smoothing*
 - *conducting materials*

■ Nano-contact measurements

- Atomic Force Microscopy (AFM)
roughness + adhesive and elastic properties
- Scanning Tunneling Microscope (STM)

Confocal microscopy



Principle of confocal microscopy
adapted from www.wikipedia.org

Surface metrology techniques

■ Stylus measurements

- Mechanical contact of a tip with surface
- Force $\geq 3\mu\text{g}$, tip radius $\geq 50\text{ nm}$
- Mainly for profile measurements $y(x)$

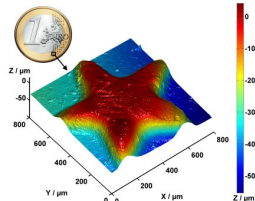
■ Optical measurements

- Confocal (laser scanning) microscopy
 - *highest lateral resolution*
- Interferometry (WLI):
 - *highest vertical resolution*
 - *10 to 100 times faster than CM*
- Scanning Electronic Microscopy (SEM):
 - *in secondary electron emission*
 - *electrons penetrate in the matter → roughness smoothing*
 - *conducting materials*

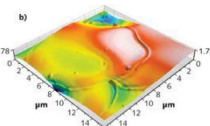
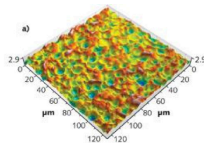
■ Nano-contact measurements

- Atomic Force Microscopy (AFM)
roughness + adhesive and elastic properties Stainless steel machined with micro-electric discharge www.laserfocusworld.org
- Scanning Tunneling Microscope (STM)

Confocal microscopy



1 euro surface www.wikipedia.org



Surface metrology techniques

■ Stylus measurements

- Mechanical contact of a tip with surface
- Force $\geq 3\mu\text{g}$, tip radius $\geq 50 \text{ nm}$
- Mainly for profile measurements $y(x)$

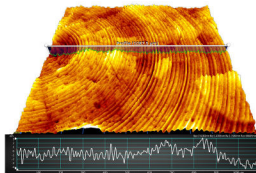
■ Optical measurements

- Confocal (laser scanning) microscopy
 - *highest lateral resolution*
- Interferometry (WLI):
 - *highest vertical resolution*
 - *10 to 100 times faster than CM*
- Scanning Electronic Microscopy (SEM):
 - *in secondary electron emission*
 - *electrons penetrate in the matter → roughness smoothing*
 - *conducting materials*

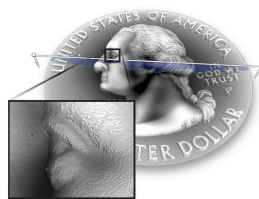
■ Nano-contact measurements

- Atomic Force Microscopy (AFM)
roughness + adhesive and elastic properties
- Scanning Tunneling Microscope (STM)

White Light Interferometry



Diamond-turned optics www.zygo.com



US quarter surface www.zygo.com

Surface metrology techniques

■ Stylus measurements

- Mechanical contact of a tip with surface
- Force $\geq 3\mu\text{g}$, tip radius $\geq 50 \text{ nm}$
- Mainly for profile measurements $y(x)$

■ Optical measurements

- Confocal (laser scanning) microscopy
- *highest lateral resolution*
- Interferometry (WLI):
- *highest vertical resolution*
- *10 to 100 times faster than CM*
- Scanning Electronic Microscopy (SEM):
- *in secondary electron emission*
- *electrons penetrate in the matter → roughness smoothing*
- *conducting materials*

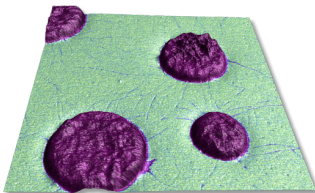
■ Nano-contact measurements

- Atomic Force Microscopy (AFM)
roughness + adhesive and elastic properties
- Scanning Tunneling Microscope (STM)

AFM



Modern AFM
www.bruker.com



Roughness and elastic moduli (color) of polymer blend
www.bruker.com

Surface metrology techniques

■ Stylus measurements

- Mechanical contact of a tip with surface
- Force $\geq 3\mu\text{g}$, tip radius $\geq 50 \text{ nm}$
- Mainly for profile measurements $y(x)$

■ Optical measurements

- Confocal (laser scanning) microscopy
 - *highest lateral resolution*
- Interferometry (WLI):
 - *highest vertical resolution*
 - *10 to 100 times faster than CM*
- Scanning Electronic Microscopy (SEM):
 - *in secondary electron emission*
 - *electrons penetrate in the matter → roughness smoothing*
 - *conducting materials*

■ Nano-contact measurements

- Atomic Force Microscopy (AFM)
roughness + adhesive and elastic properties
- Scanning Tunneling Microscope (STM)

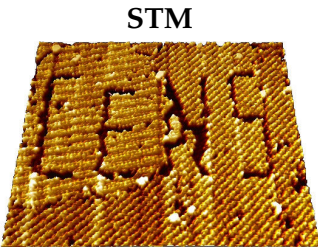
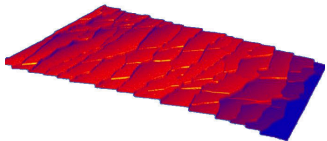


Fig. Center for NanoScience logo imprinted at atomic scale

www.cens.de



Atomic steps on platinum surface
(500×500 nm)

www.icryst.com

Roughness: classification

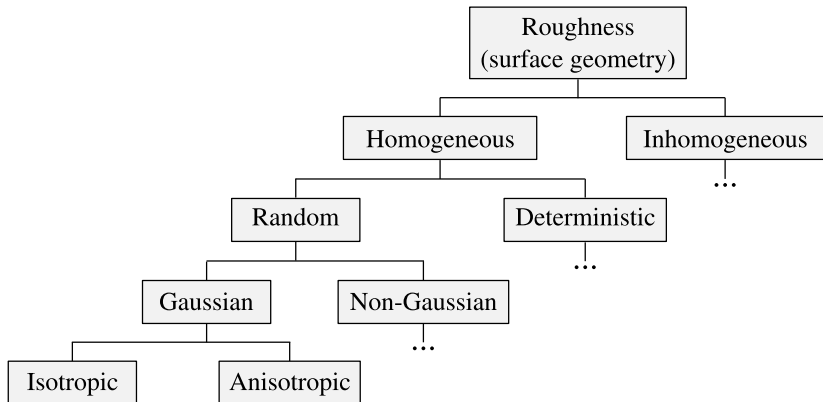


Fig. Roughness classification according to Nayak^[1]

[1] Nayak, J. Lub. Tech. (ASME) 93:398 (1971)

Roughness: classification

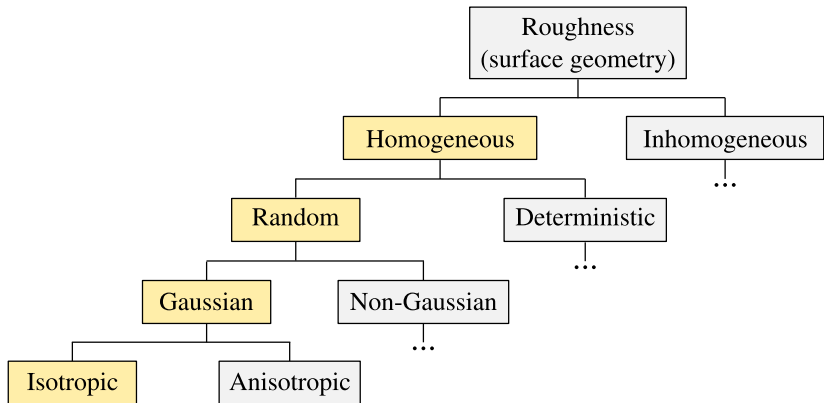


Fig. Roughness classification according to Nayak^[1]

[1] Nayak, J. Lub. Tech. (ASME) 93:398 (1971)

Roughness and geometry/form

- Roughness vs geometry of surfaces
- Sometimes macroscopic geometry is subtracted (filtered out):
form → error of form → waviness → roughness
- Non-trivial to remove macroscopic shape
- Most roughness measurement tools enable shape removal

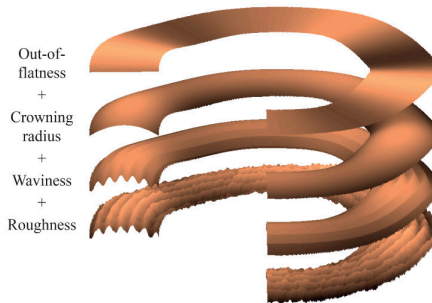


Fig. Circular metallic seal with turned copper surface^[1]

[1] F.P. Rafols, Licentiate Thesis, LTU 2016.

Roughness and geometry/form

- Roughness vs geometry of surfaces
- Sometimes macroscopic geometry is subtracted (filtered out):
form→error of form→waviness→roughness
- Non-trivial to remove macroscopic shape
- Most roughness measurement tools enable shape removal

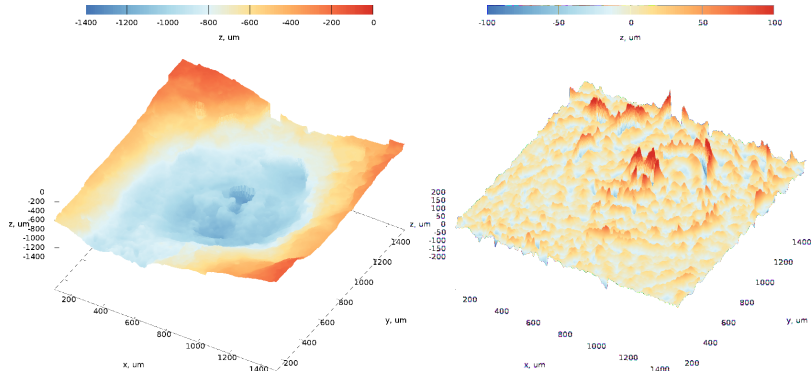


Fig. (left) impact crater, (right) shape is filtered out

Roughness and geometry/form

- Roughness vs geometry of surfaces
- Sometimes macroscopic geometry is subtracted (filtered out):
form→error of form→waviness→roughness
- Non-trivial to remove macroscopic shape
- Most roughness measurement tools enable shape removal

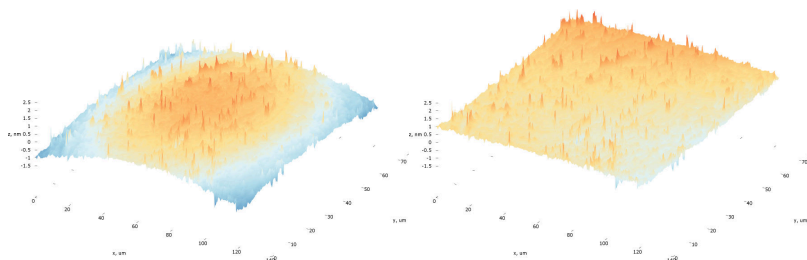


Fig. (left) spherical indenter, (right) $z = a(x^2 + y^2)$ shape is subtracted

Main characteristics

Integral quantities

- Average of absolute values [l.u.] (profile - R_a , surface - S_a)

$$S_a = \frac{1}{A} \int_A |z(x, y) - \bar{z}| dA, \quad S_a = \frac{1}{N^2} \sum_{i=1}^N \sum_{j=1}^N |z_{ij} - \bar{z}|$$

- Standard deviation of height [l.u.] (σ or R_q for profile, S_q for surface)

$$\sigma = \sqrt{\frac{1}{A} \int_A (z(x, y) - \bar{z})^2 dA}, \quad \sigma = \frac{1}{N} \sqrt{\sum_{i=1}^N \sum_{j=1}^N (z_{ij} - \bar{z})^2}$$

- Maximal valley depth R_v, S_v , maximal peak height R_p, S_p [l.u.]
very sensitive to sample area
- Skewness [adim] (γ_1 or R_{sk}, S_{sk})

$$\gamma_1 = \frac{1}{A\sigma^3} \int_A (z(x, y) - \bar{z})^3 dA, \quad \gamma_1 = \frac{1}{N^2\sigma^3} \sum_{i=1}^N \sum_{j=1}^N (z_{ij} - \bar{z})^3$$

- Kurtosis [adim] (κ or R_{ku}, S_{ku})

$$\kappa = \frac{1}{A\sigma^4} \int_A (z(x, y) - \bar{z})^4 dA, \quad \kappa = \frac{1}{N^2\sigma^4} \sum_{i=1}^N \sum_{j=1}^N (z_{ij} - \bar{z})^4$$

Main characteristics II

Integral quantities II

- Average of absolute value of gradient (slope) [adim] (profile - R_{dq} , surface - S_{dq})

$$S_{da} = \langle |\nabla z(x, y) - \bar{\nabla}z| \rangle = \frac{1}{A} \int_A |\nabla z(x, y) - \bar{\nabla}z| dA$$
$$S_{da} = \frac{1}{N^2} \sum_{i=1}^N \sum_{j=1}^N \left| \frac{z_{i+1,j} - z_{i,j} - \bar{\Delta}z_x}{\Delta x} \right| + \left| \frac{z_{i,j+1} - z_{i,j} - \bar{\Delta}z_y}{\Delta y} \right|$$

- Standard deviation of gradient (slope) [adim] (profile - R_{dq} , surface - S_{dq})

$$S_{dq} = \sqrt{\langle |\nabla z(x, y) - \bar{\nabla}z|^2 \rangle} = \sqrt{\frac{1}{A} \int_A |\nabla z(x, y) - \bar{\nabla}z|^2 dA}$$

$$S_{dq} = \sqrt{\frac{1}{N^2} \sum_{i=1}^N \sum_{j=1}^N \left| \frac{z_{i+1,j} - z_{i,j} - \bar{\Delta}z_x}{\Delta x} \right|^2 + \left| \frac{z_{i,j+1} - z_{i,j} - \bar{\Delta}z_y}{\Delta y} \right|^2}$$

- Often in integrated slope measurements a smoothing filter is used, for example, according to ASME B46.1 standard

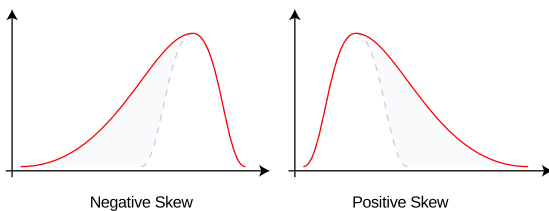
$$\frac{\partial z}{\partial x} \approx \frac{1}{60\Delta x} (z_{i+3,j} - 9z_{i+2,j} + 45z_{i+1,j} - 45z_{i-1,j} + 9z_{i-2,j} - z_{i-3,j})$$

Main characteristics: probability density

- Probability density of heights $P(z)$
- Properties and moments

$$1 = \int_{-\infty}^{\infty} P(z) dz, \quad \bar{z} = \int_{-\infty}^{\infty} zP(z) dz, \quad \sigma = \sqrt{\int_{-\infty}^{\infty} (z - \bar{z})^2 P(z) dz}$$
$$\mu_q = \int_{-\infty}^{\infty} z^q P(z) dz \quad \text{then} \quad \mu_0 = 1, \mu_1 = \bar{z}, \mu_2 = \sigma^2 + \bar{z}^2$$

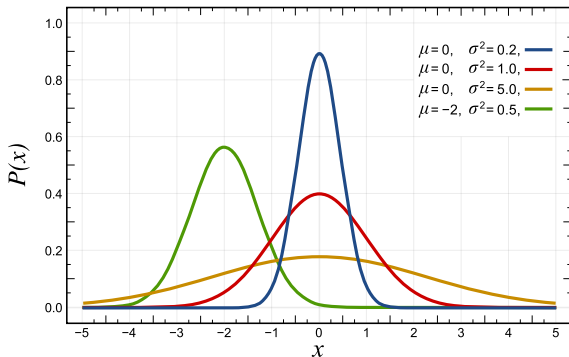
- Link to skewness



Main characteristics: probability density II

Distribution examples

- Normal (Gaussian): $P(x) = \frac{1}{\sigma \sqrt{2\pi}} \exp\left[-\frac{(x - \mu_1)^2}{2\sigma^2}\right], x \in \mathbb{R}$

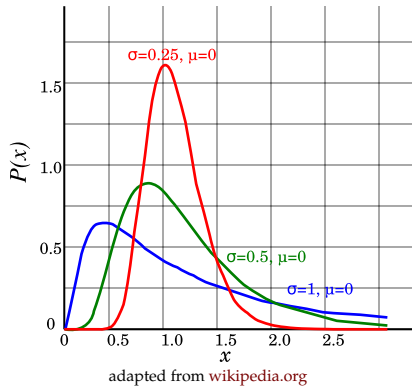


adapted from [wikipedia.org](https://en.wikipedia.org)

Main characteristics: probability density II

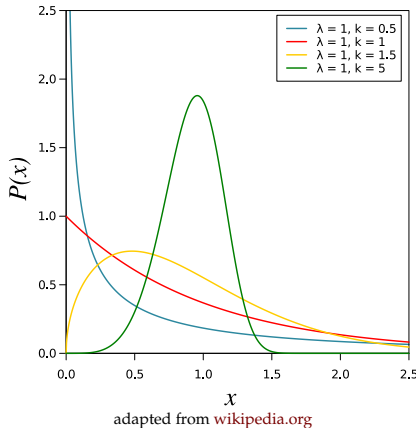
Distribution examples

■ Lognormal: $P(x) = \frac{1}{x\sigma\sqrt{2\pi}} \exp\left[-\frac{(\log(x) - \mu_1)^2}{2\sigma^2}\right] x \in \mathbb{R}^+$



Distribution examples

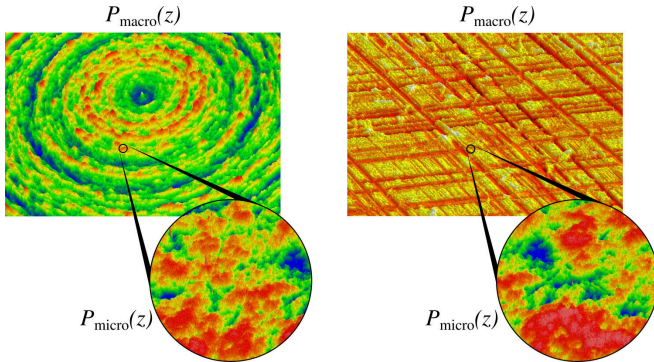
- Weibull: $P(x) = \frac{k}{\lambda} \left(\frac{x}{\lambda}\right)^{k-1} \exp(-(x/\lambda)^k) \quad x \in \mathbb{R}^+$



adapted from [wikipedia.org](https://en.wikipedia.org)

Real rough surfaces

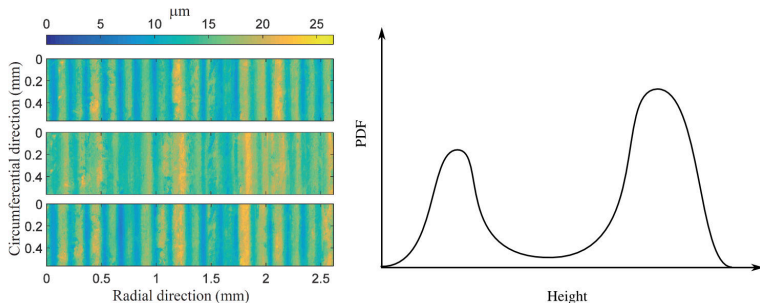
- Turning, scratching, shaping changes macroscopic distribution P_{macro} but might keep microscopic distribution intact P_{micro}
- Wear, polishing, flattening results in removal of the right distribution tail $P(z > z_0) \rightarrow 0$: negative kurtosis



Macro- and microscopic roughness (left: diamond-turned surface, right: cross-hatched surface)
Images from www.zygo.com used

Real rough surfaces

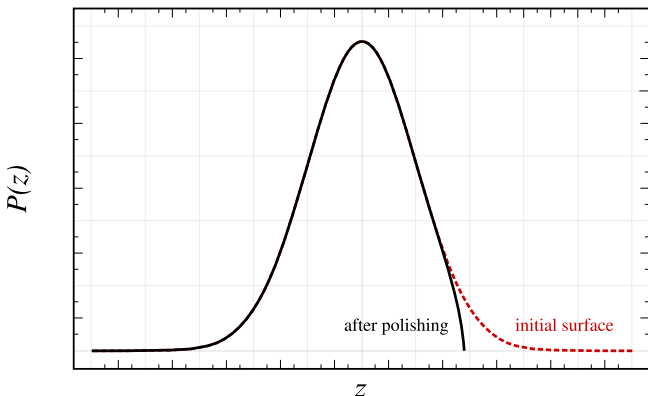
- Turning, scratching, shaping changes macroscopic distribution P_{macro} but might keep microscopic distribution intact P_{micro}
- Wear, polishing, flattening results in removal of the right distribution tail $P(z > z_0) \rightarrow 0$: negative kurtosis



Turned surface topography and a sketch of height PDF
Pérez-Ràfols, Larsson, Almqvist, Tribol Int 94 (2016)

Real rough surfaces

- Turning, scratching, shaping changes macroscopic distribution P_{macro} but might keep microscopic distribution intact P_{micro}
- Wear, polishing, flattening results in removal of the right distribution tail $P(z > z_0) \rightarrow 0$: negative kurtosis



Initial surface with Gaussian PDF and surface after polishing

Real rough surfaces

- Turning, scratching, shaping changes macroscopic distribution P_{macro} but might keep microscopic distribution intact P_{micro}
- Wear, polishing, flattening results in removal of the right distribution tail $P(z > z_0) \rightarrow 0$: negative curtosis



Very fresh asphalt concrete



Normal asphalt concrete

Real rough surfaces

- Turning, scratching, shaping changes macroscopic distribution P_{macro} but might keep microscopic distribution intact P_{micro}
- Wear, polishing, flattening results in removal of the right distribution tail $P(z > z_0) \rightarrow 0$: negative curtosis



Very fresh asphalt concrete



Normal asphalt concrete . . . with a bolt ☺

Real rough surfaces

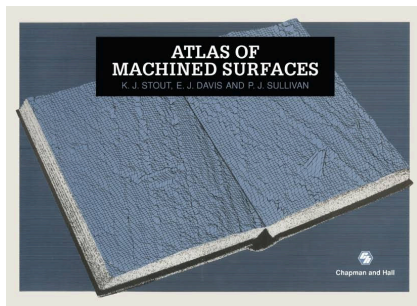
- Turning, scratching, shaping changes macroscopic distribution P_{macro} but might keep microscopic distribution intact P_{micro}
- Wear, polishing, flattening results in removal of the right distribution tail $P(z > z_0) \rightarrow 0$: negative curtosis



Old asphalt concrete with worn out bitumen

Real rough surfaces

- Turning, scratching, shaping changes macroscopic distribution P_{macro} but might keep microscopic distribution intact P_{micro}
- Wear, polishing, flattening results in removal of the right distribution tail $P(z > z_0) \rightarrow 0$: negative curtosis



Atlas of machined surfaces (with height distributions)

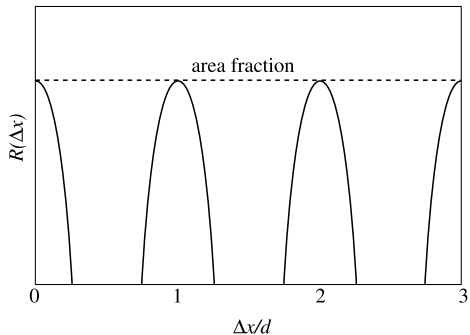
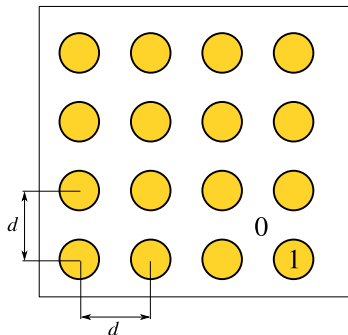
Autocorrelation function

- Continuous autocorrelation function

$$R(\Delta x, \Delta y) = \lim_{L \rightarrow \infty} \frac{1}{L^2} \int_0^L \int_0^L z(x + \Delta x, y + \Delta y) z(x, y) dx dy$$

- Discrete autocorrelation function for a surface $N \times N$

$$R(\Delta x, \Delta y) = \frac{1}{N^2} \sum_{i=0}^{N-1} \sum_{j=0}^{N-1} z(x + \Delta x, y + \Delta y) z(x, y)$$



Power spectral density (PSD)

- Recall: Fourier Transform: $\hat{f}(k) = \int_{-\infty}^{\infty} f(x) \exp(-2\pi i k x) dx$
- Recall: Discrete Fourier Transform: $\hat{f}_k = \sum_{n=0}^{N-1} x_n \exp(-2\pi i k n / N)$
- where x is the spatial coordinate, $k = 2\pi/\lambda$ is the wavenumber and λ is the wavelength.
- PSD is the Fourier Transform of R
$$\Phi(k_x, k_y) \equiv \hat{R}(k_x, k_y) = \text{FFT} [z(x + \Delta x, y + \Delta y) * z(x, y)]$$
- Using convolution theorem
$$\Phi(k_x, k_y) = \hat{z}(k_x, k_y) \hat{z}^*(k_x, k_y) = \hat{z}^2(k_x, k_y)$$
- Interpretation: energy distribution by frequencies
- Usage: signal analysis, seismology, microstructure characterization, roughness.

Spectral moments

- Spectral moment m_{pq} , $p, q \in \mathbb{N}$:

$$m_{pq} = \iint_{-\infty}^{\infty} k_x^p k_y^q \Phi(k_x, k_y) dk_x dk_y$$

$$m_{pq} = \left[\frac{2\pi}{L} \right]^{p+q} \sum_{i=0}^{N-1} \sum_{j=0}^{N-1} i^p j^q \Phi(2\pi i/L, 2\pi j/L)$$

- Generalized spectral moment m_{pq} , $p, q \in \mathbb{R}^+$
- For isotropic surface: $m_2 = m_{20} = m_{02}$, $m_4 = 3m_{22} = m_{40} = m_{04}$
- Averaging:

$$m_2 = \frac{m_{20} + m_{02}}{2}, \quad m_4 = \frac{m_{40} + 3m_{22} + m_{04}}{3}$$

- Physical meaning:

Height variance¹: $m_0 = \langle (z - \langle z \rangle)^2 \rangle$

Gradient variance: $2m_2 = \langle (\nabla z - \langle \nabla z \rangle)^2 \rangle$

Curvature variance: $m_4 = \langle (\nabla \cdot \nabla z - \langle \nabla \cdot \nabla z \rangle)^2 \rangle$

¹Variance is a squared standard deviation

Summary

- Fractal (self-affine) roughness
- Power spectral density (PSD)
 $\Phi(k) \sim k^{-2(H+1)}$

k is a wavenumber,
H is the Hurst exponent.
- Isotropic/anisotropic surfaces
- Gaussian/non-Gaussian height distribution $P(h)$

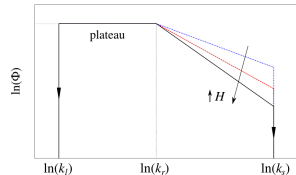
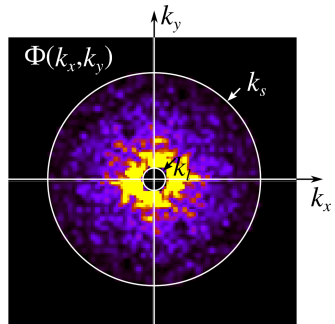


Fig. 3D and radial power spectral densities

Summary

- Fractal (self-affine) roughness
- Power spectral density (PSD)
 $\Phi(k) \sim k^{-2(H+1)}$

k is a wavenumber,
 H is the Hurst exponent.
- Isotropic/anisotropic surfaces
- Gaussian/non-Gaussian height distribution $P(h)$

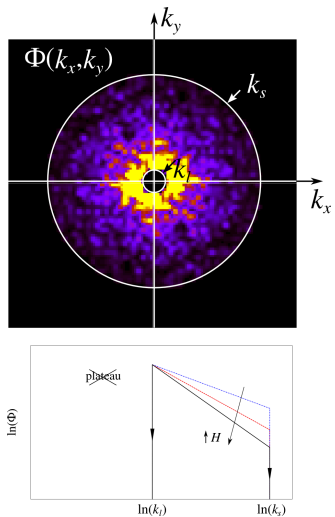


Fig. 3D and radial power spectral densities

Summary

- Fractal (self-affine) roughness
- Power spectral density (PSD)
 $\Phi(k) \sim k^{-2(H+1)}$

k is a wavenumber,

H is the Hurst exponent.

- Isotropic/anisotropic surfaces
- Gaussian/non-Gaussian height distribution $P(h)$

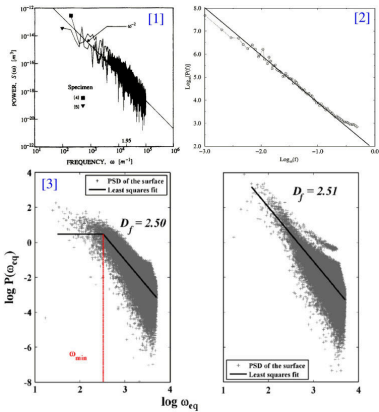


Fig. Power spectral density, measurements

[1] Majumdar, Tien, Wear 136 (1990)

[2] Schmittbuhl, Jørgen Måløy, Phys. Rev. Lett. 78 (1997)

[3] Vallet, Lasseux, Sainsot, Zahouani, Tribol. Int. 42 (2009)

Summary

- Fractal (self-affine) roughness
- Power spectral density (PSD)
$$\Phi(k) \sim k^{-2(H+1)}$$

k is a wavenumber,
H is the Hurst exponent.
- Isotropic/anisotropic surfaces
- Gaussian/non-Gaussian height distribution $P(h)$

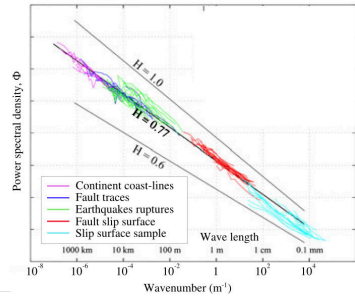


Fig. Power spectral density, geological scales

Adapted from

[4] Renard, Candela, Bouchaud, Geophys. Res. Lett. 40 (2013)

Summary

- Fractal (self-affine) roughness
- Power spectral density (PSD)
 $\Phi(k) \sim k^{-2(H+1)}$

k is a wavenumber,
 H is the Hurst exponent.
- Isotropic/anisotropic surfaces
- Gaussian/non-Gaussian height distribution $P(h)$

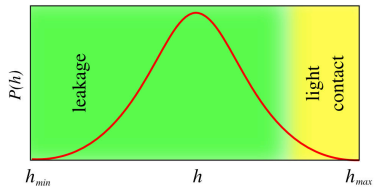


Fig. Height distribution $P(h)$

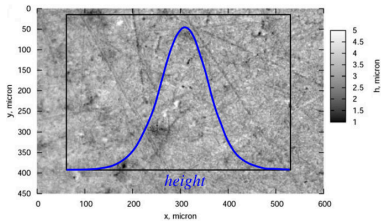


Fig. Height distribution of a polished metal surface

Summary

- Fractal (self-affine) roughness
- Power spectral density (PSD)
$$\Phi(k) \sim k^{-2(H+1)}$$

k is a wavenumber,
 H is the Hurst exponent.

- Isotropic/anisotropic surfaces
- Gaussian/non-Gaussian height distribution $P(h)$
- Characteristics:

- $\sqrt{\langle z^2 \rangle}$ - rms heights
- $\sqrt{\langle |\nabla z|^2 \rangle}$ - rms slope (surface gradient)
- $\alpha = m_{00}m_{40}/m_{20}^2$ - breadth of the spectrum (Nayak's parameter^[B]),

$$\text{spectral moments } m_{pq} = \iint_{-\infty}^{\infty} k_x^p k_y^q \Phi(k_x, k_y) dk_x dk_y$$

■ Random process theory

[A] Longuet-Higgins, Philos. Trans. R. Soc. A 250:157 (1957)

[B] Nayak, J. Lub. Tech. (ASME) 93:398 (1973)

[C] Greenwood, Wear 261: 191 (2006)

[D] Borri, Paggi, J. Phys. D Appl Phys 48:045301 (2015)

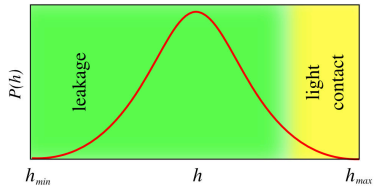


Fig. Height distribution $P(h)$

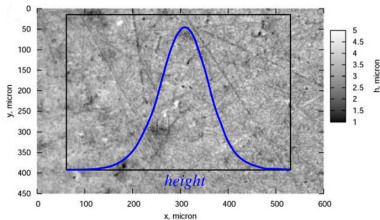


Fig. Height distribution of a polished metal surface

Summary

- Fractal (self-affine) roughness
- Power spectral density (PSD)
$$\Phi(k) \sim k^{-2(H+1)}$$

k is a wavenumber,
 H is the Hurst exponent.

- Isotropic/anisotropic surfaces
- Gaussian/non-Gaussian height distribution $P(h)$
- Characteristics:

- $\sqrt{\langle z^2 \rangle}$ - rms heights
- $\sqrt{\langle |\nabla z|^2 \rangle}$ - rms slope (surface gradient)
- $\alpha = m_{00}m_{40}/m_{20}^2$ - breadth of the spectrum (Nayak's parameter^[B]),

$$\text{spectral moments } m_{pq} = \iint_{-\infty}^{\infty} k_x^p k_y^q \Phi(k_x, k_y) dk_x dk_y$$

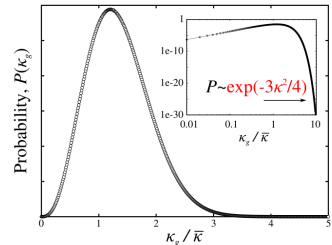
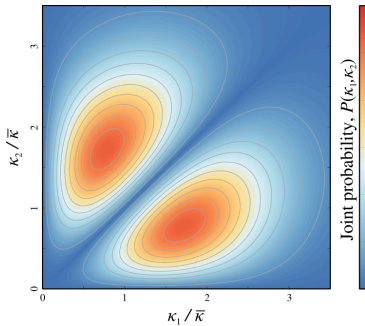
■ Random process theory

[A] Longuet-Higgins, Philos. Trans. R. Soc. A 250:157 (1957)

[B] Nayak, J. Lub. Tech. (ASME) 93:398 (1973)

[C] Greenwood, Wear 261: 191 (2006)

[D] Borri, Paggi, J. Phys. D Appl. Phys 48:045301 (2015)



$$P \sim \kappa^2 \exp(-3\kappa^2/4) \operatorname{erf}(3\kappa/2)$$

Distribution of asperity curvatures

Summary

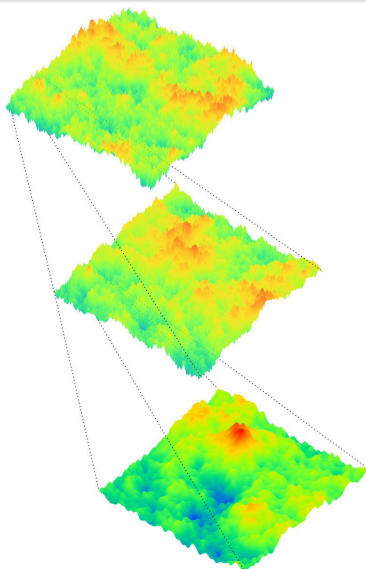


Fig. Example of a rough surface for $H = 0.3$

Recall: the Hurst exponent H and the fractal dimension D in 2D space are interconnected via $D = 3 - H$

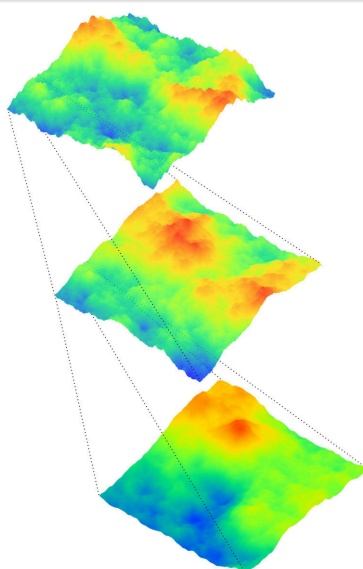
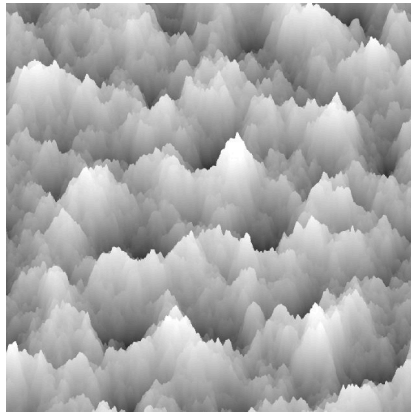


Fig. Example of a rough surface for $H = 0.8$

Fractals



Flight over a rough surface

Fractals

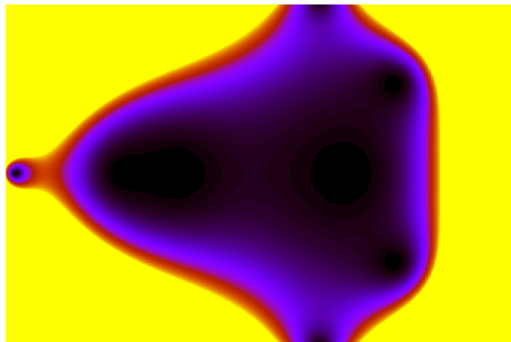


Romanesco broccoli www.fourmilab.ch

Fractals

- Mandelbrot set (not a fractal)
- Recursive function

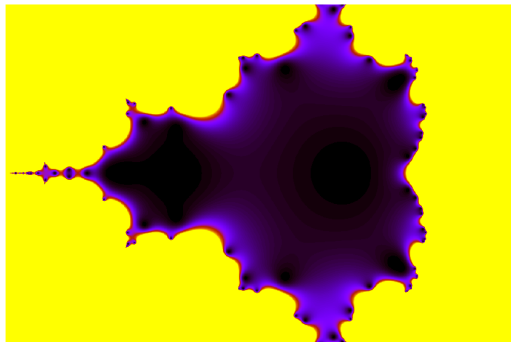
$$z_{i+1} = z_i^2 + z, \quad z \in \mathbb{C}$$



Fractals

- Mandelbrot set (not a fractal)
- Recursive function

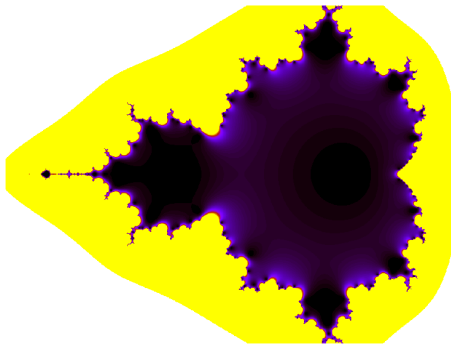
$$z_{i+1} = z_i^2 + z, \quad z \in \mathbb{C}$$



Fractals

- Mandelbrot set (not a fractal)
- Recursive function

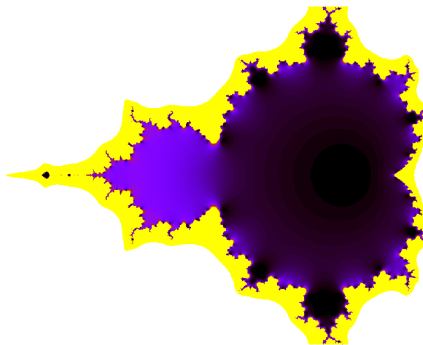
$$z_{i+1} = z_i^2 + z, \quad z \in \mathbb{C}$$



Fractals

- Mandelbrot set (not a fractal)
- Recursive function

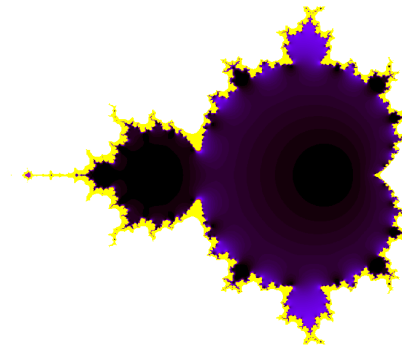
$$z_{i+1} = z_i^2 + z, \quad z \in \mathbb{C}$$



Fractals

- Mandelbrot set (not a fractal)
- Recursive function

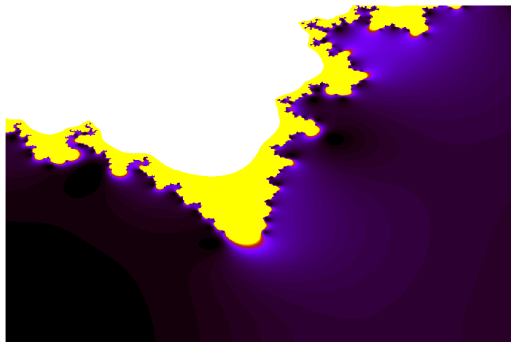
$$z_{i+1} = z_i^2 + z, \quad z \in \mathbb{C}$$



Fractals

- Mandelbrot set (not a fractal)
- Recursive function

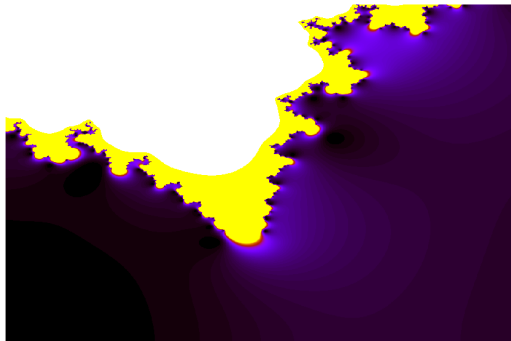
$$z_{i+1} = z_i^2 + z, \quad z \in \mathbb{C}$$



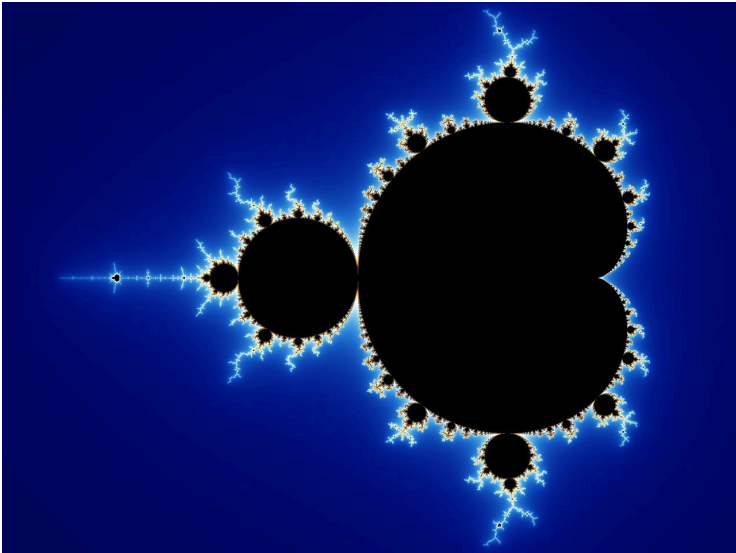
Fractals

- Mandelbrot set (not a fractal)
- Recursive function

$$z_{i+1} = z_i^2 + z, \quad z \in \mathbb{C}$$

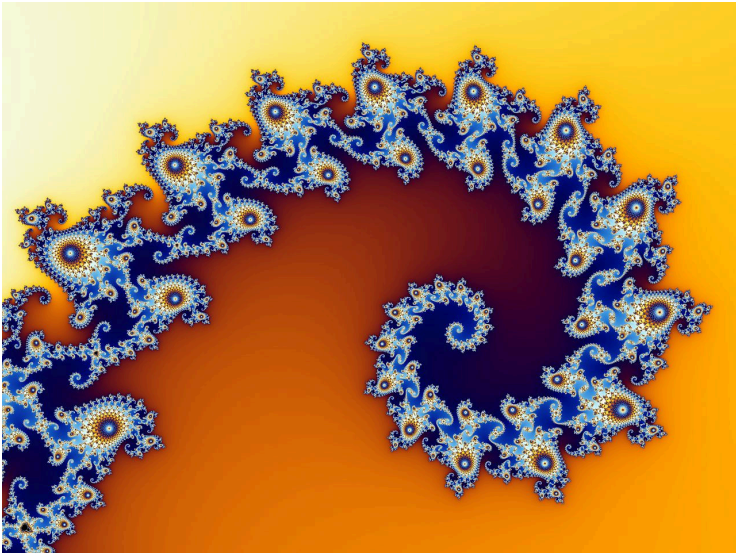


Fractals



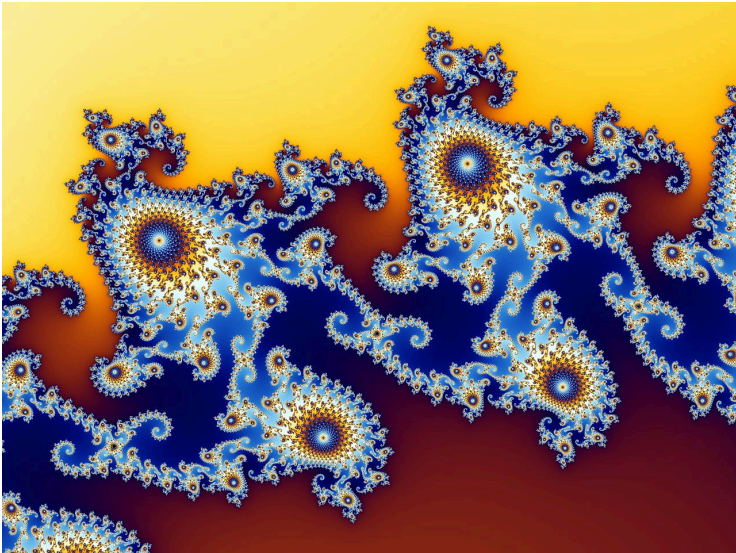
Mandelbrot set ([Wikipedia](#))

Fractals



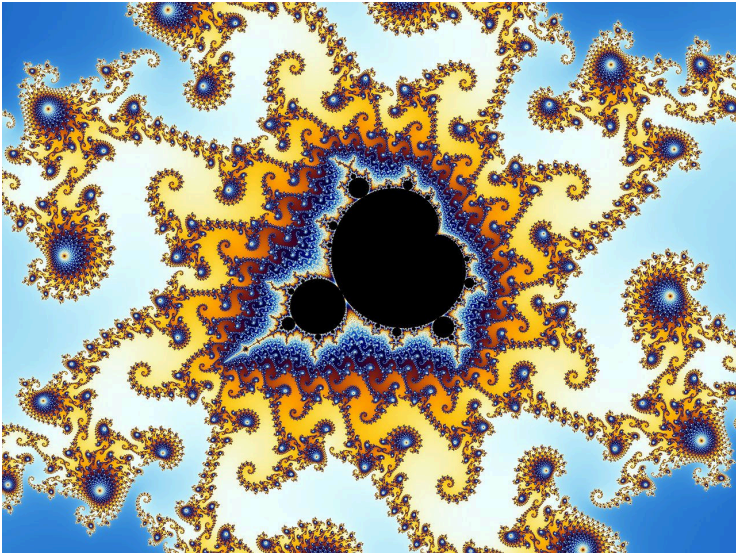
Element of Mandelbrot set ([Wikipedia](#))

Fractals



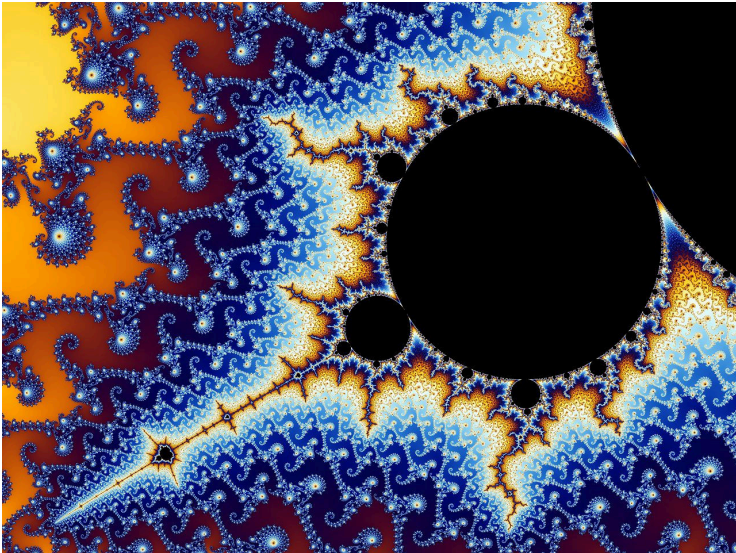
Element of Mandelbrot set ([Wikipedia](#))

Fractals



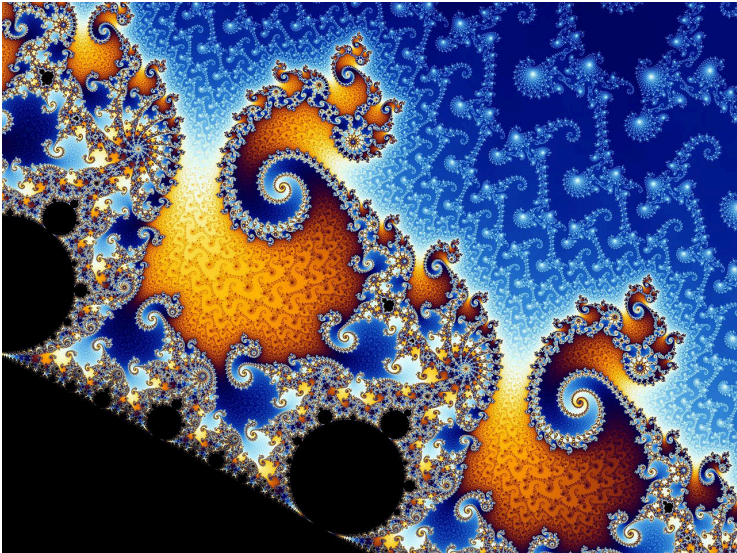
Element of Mandelbrot set ([Wikipedia](#))

Fractals



Element of Mandelbrot set ([Wikipedia](#))

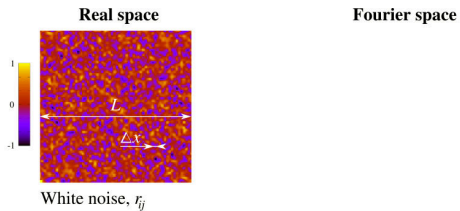
Fractals



Element of Mandelbrot set ([Wikipedia](#))

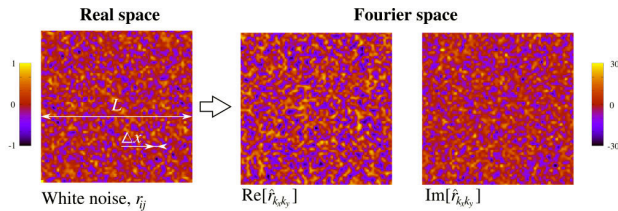
Animation

Synthesized rough surfaces: in pictures



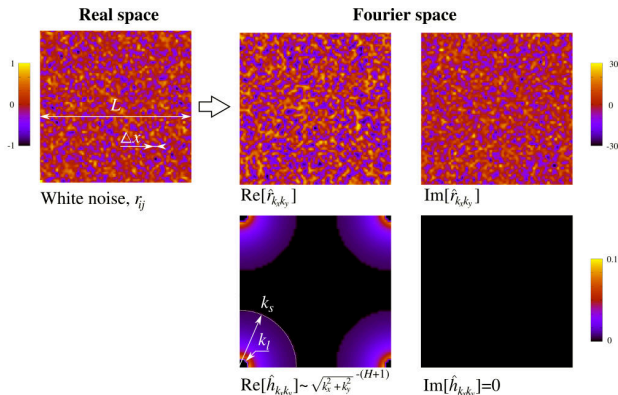
[1] Y. Z. Hu and K. Tonder, Int. J. Machine Tools Manuf. 32, 83 (1992)

Synthesized rough surfaces: in pictures



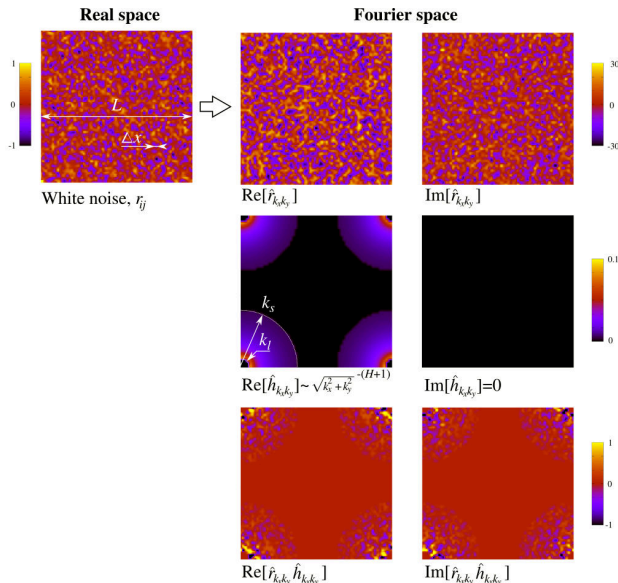
[1] Y. Z. Hu and K. Tonder, Int. J. Machine Tools Manuf. 32, 83 (1992)

Synthesized rough surfaces: in pictures



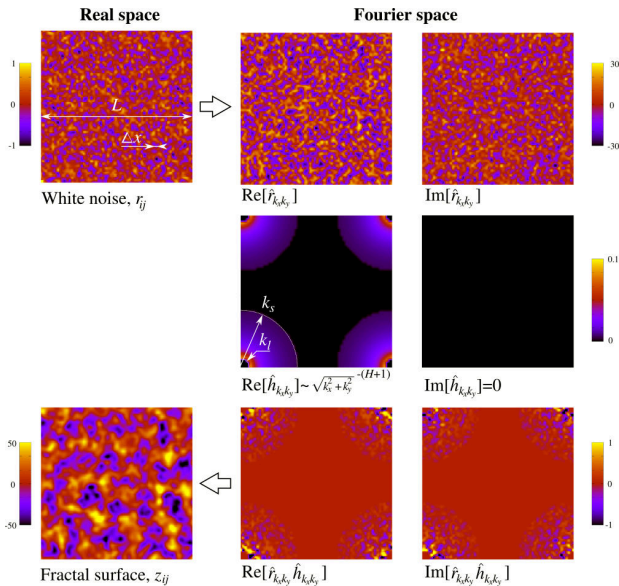
[1] Y. Z. Hu and K. Tonder, Int. J. Machine Tools Manuf. 32, 83 (1992)

Synthesized rough surfaces: in pictures



[1] Y. Z. Hu and K. Tonder, Int. J. Machine Tools Manuf. 32, 83 (1992)

Synthesized rough surfaces: in pictures



[1] Y. Z. Hu and K. Tonder, Int. J. Machine Tools Manuf. 32, 83 (1992)

Synthesized rough surfaces: in equations

- White noise:

$$w(x_i, y_j), \quad \langle w \rangle = 0, \quad \langle w^2 \rangle = \Phi_0$$

- Transform in Fourier space:

$$\hat{w}_{ij} = \hat{w}(k_x, k_y) = \sum_{i=0}^{N-1} \sum_{j=0}^{N-1} w(x_i, y_j) \exp[-i(k_x x_i + k_y y_j)], \quad \langle \hat{w} \hat{w}^* \rangle = \langle w^2 \rangle = \Phi_0$$

- Create a filter

$$\hat{f}_{ij} = \hat{f}(k_x, k_y) = \begin{cases} \left[\frac{K_x^2 + K_y^2}{k_l^2} \right]^{-(1+H)/2}, & \text{for } 1 \leq \frac{\sqrt{K_x^2 + K_y^2}}{k_l} \leq \zeta \\ 0, & \text{elsewhere,} \end{cases},$$

- Where $K_x = (s+1)\pi/L - sk_x$, $K_y = (t+1)\pi/L - tk_y$ for $s, t \in \{-1, 1\}$, $\zeta = k_s/k_l$

$$\hat{z}_{ij} = \hat{z}(k_x, k_y) = \Re(\hat{f}_{ij}) [\Re(\hat{w}_{ij}) + i \Im(\hat{w}_{ij})]$$

- Back to real space:

$$z(x_i, y_j) = \sum_{l=0}^{N-1} \sum_{m=0}^{N-1} \hat{z}_{lm} \exp[i2\pi(lx_i + my_j)/L]$$

Synthesized rough surfaces: in equations II

- Power spectral density:

$$\Phi(k_x, k_y) = \hat{z}(k_x, k_y)\hat{z}^*(k_x, k_y) = \hat{f}^2(k_x, k_y)\hat{w}^2(k_x, k_y)$$

- Averaging over multiple samples:

$$\langle \Phi(k_x, k_y) \rangle = \langle \hat{w}^2(k_x, k_y) \rangle \hat{f}^2(k_x, k_y) = \begin{cases} \Phi_0 \left[\frac{\sqrt{k_x^2 + k_y^2}}{k_l} \right]^{-2(1+H)}, & \text{for } 1 \leq \frac{\sqrt{k_x^2 + k_y^2}}{k_l} \leq \zeta \\ 0, & \text{elsewhere,} \end{cases}$$

- For isotropic surface:

$$\langle \Phi(K) \rangle = \begin{cases} \Phi_0(K/k_l)^{-2(1+H)}, & \text{if } 1 \leq K/k_l \leq \zeta \\ 0, & \text{otherwise.} \end{cases}$$

Effect of parameters: illustration

- Effect of the high frequency cutoff k_s

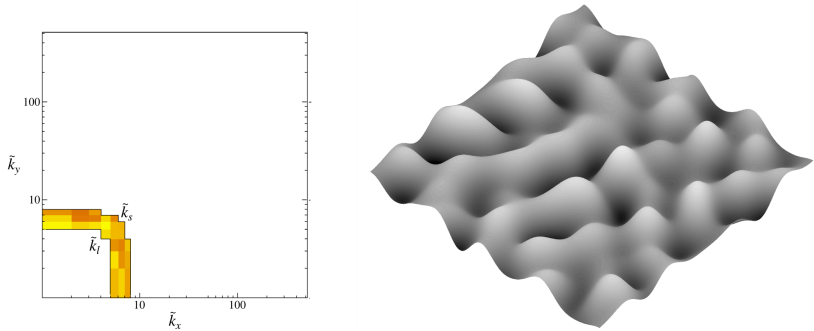


Fig. Power spectral density (Fourier space)
and corresponding rough surface (real space) for
 $k_l = 4, k_s = 8$

Effect of parameters: illustration

- Effect of the high frequency cutoff k_s

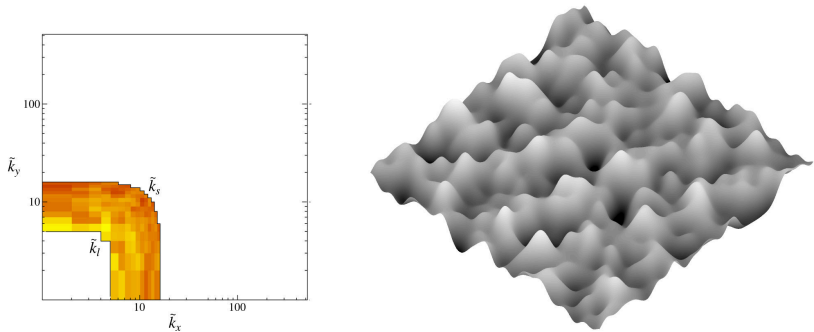


Fig. Power spectral density (Fourier space)
and corresponding rough surface (real space) for
 $k_l = 4, k_s = 16$

Effect of parameters: illustration

- Effect of the high frequency cutoff k_s

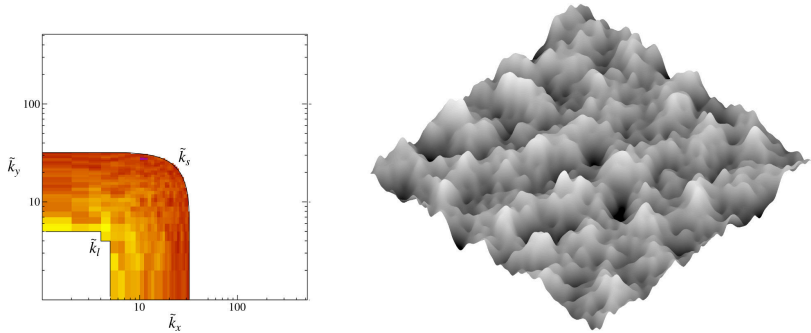


Fig. Power spectral density (Fourier space)
and corresponding rough surface (real space) for
 $k_l = 4, k_s = 32$

Effect of parameters: illustration

- Effect of the high frequency cutoff k_s

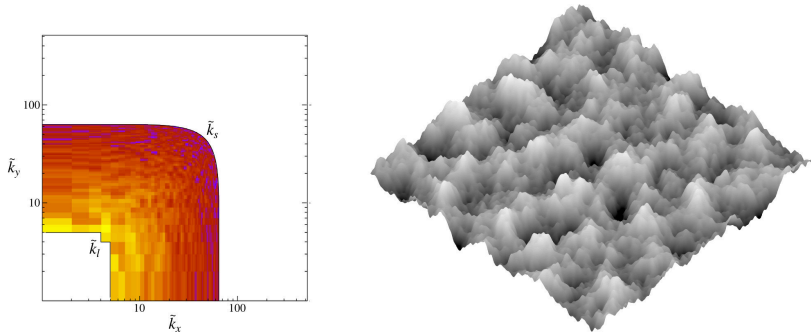


Fig. Power spectral density (Fourier space)
and corresponding rough surface (real space) for
 $k_l = 4, k_s = 64$

Effect of parameters: illustration

- Effect of the high frequency cutoff k_s

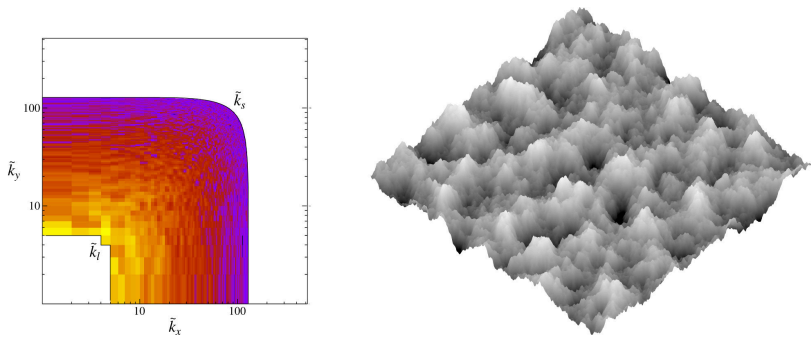


Fig. Power spectral density (Fourier space)
and corresponding rough surface (real space) for
 $k_l = 4, k_s = 128$

Effect of parameters: illustration

- Effect of the lower frequency cutoff k_l for $k_s/k_l = \text{const}$

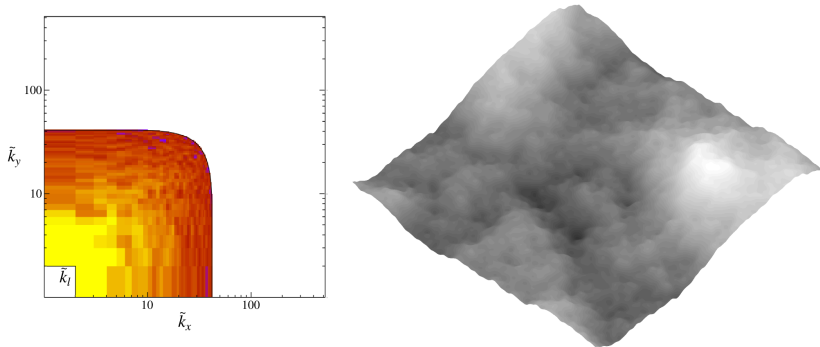


Fig. Power spectral density (Fourier space)
and corresponding rough surface (real space) for
 $k_l = 1, k_s = 43$

Effect of parameters: illustration

- Effect of the lower frequency cutoff k_l for $k_s/k_l = \text{const}$

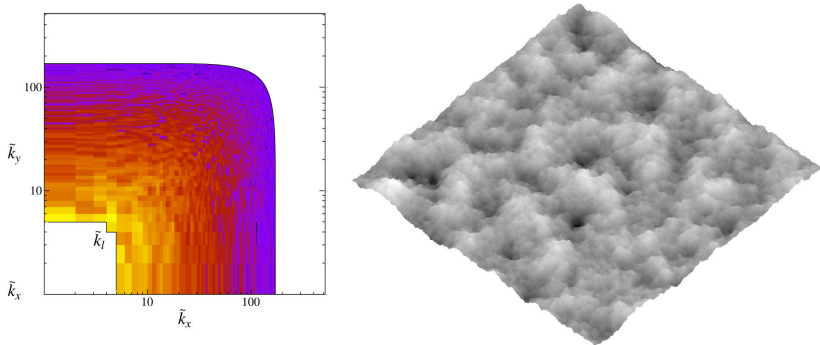


Fig. Power spectral density (Fourier space)
and corresponding rough surface (real space) for
 $k_l = 4, k_s = 171$

Effect of parameters: illustration

- Effect of the lower frequency cutoff k_l for $k_s/k_l = \text{const}$

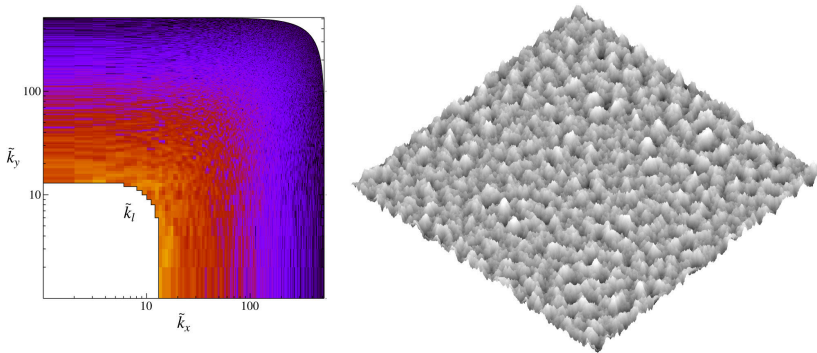


Fig. Power spectral density (Fourier space)
and corresponding rough surface (real space) for
 $k_l = 12, k_s = 512$

Effect of parameters: illustration

- Effect of the ratio of the higher cutoff to the discretization k_s/N

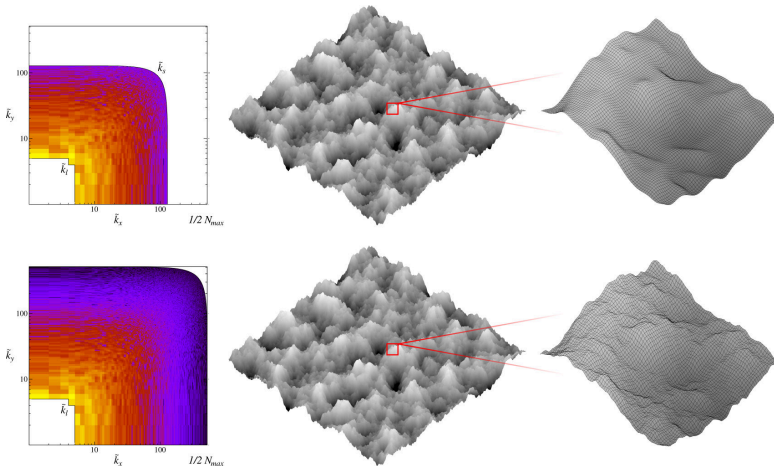


Fig. Power spectral densities (Fourier space)
and corresponding rough surfaces (real space) for
 $k_l = 12, k_s/N = 1/8$ VS $k_l = 12, k_s/N = 1/2$

Effect of parameters: illustration

- Effect of the ratio of the higher cutoff to the discretization k_s/N

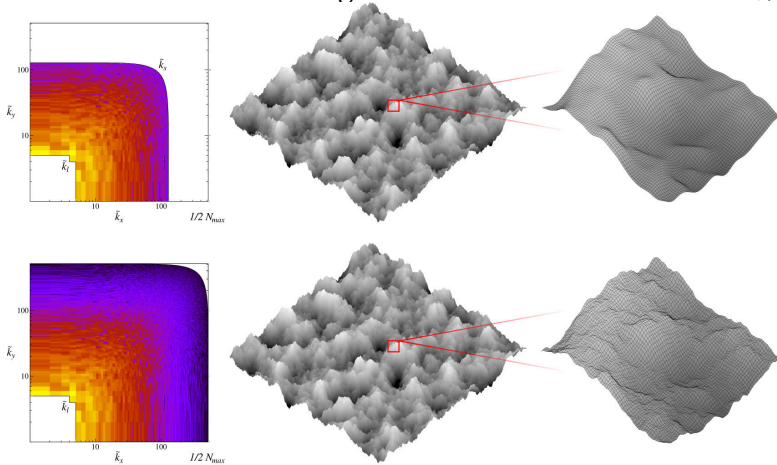


Fig. Power spectral densities (Fourier space) and corresponding rough surfaces (real space) for
 $k_l = 12$, $k_s/N = 1/8$ (fine) VS $k_l = 12$, $k_s/N = 1/2$ (too coarse)
for mechanical simulations

Effect of parameters: illustration

- Effect of the discretisation (single asperity)

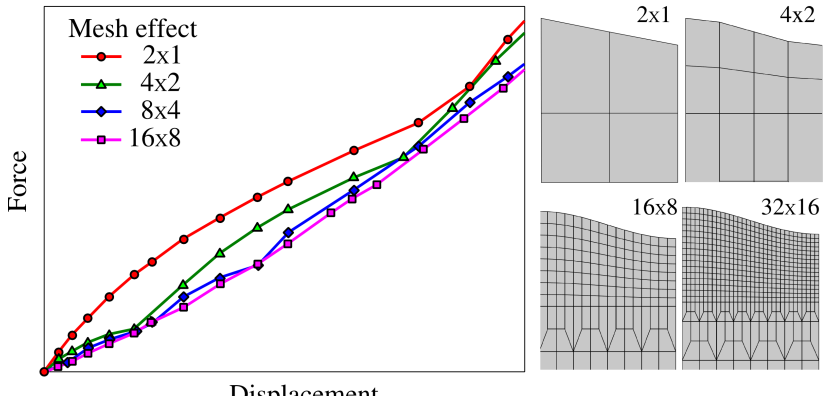


Fig. Effect of the mesh on mechanical response

Effect of parameters: illustration

- Data interpolation (Shanon, bi-cubic Bézier surfaces)

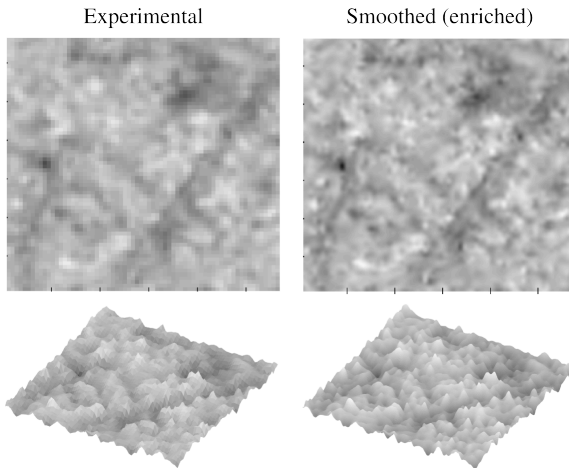


Fig. Bi-cubic Bézier interpolation of an experimental rough surface

[1] Hyun, Robbins, Tribol. Int. (2007)

[2] Yastrebov, Durand, Proudhon, Cailletaud, C.R. Mécan. (2011)

Effect of parameters

Effect of parameters:

- k_l low frequency cutoff
 - *representativity/normality*^[1,2,3]
- k_s high frequency cutoff
 - *smoothness and density of asperities*
- $\zeta = k_s/k_l$ ratio^[3]
 - *breadth of the spectrum*

$$\alpha \sim \zeta^{2H}$$

Nayak's parameter α is the central characteristic of roughness in asperity based mechanical models.

- [1] Vallet, Lasseux, Sainsot, Zahouani, Tribol. Int. (2009)
- [2] Yastrebov, Durand, Proudhon, Cailletaud, C.R. Mécan. (2011)
- [3] Yastrebov, Anciaux, Molinari, Phys. Rev. E (2012)
- [4] Yastrebov, Anciaux, Molinari, Int. J. Solids Struct. (2015)

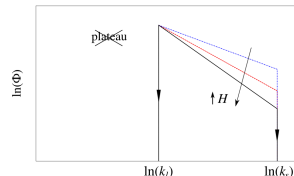
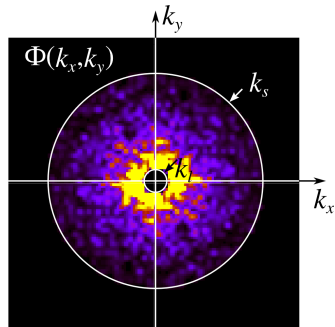


Fig. 3D and radial power spectral densities

Effect of parameters

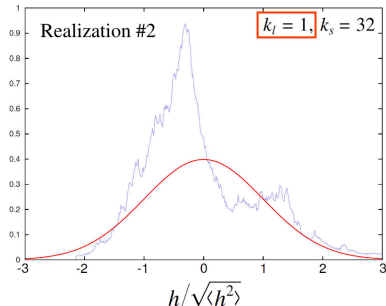
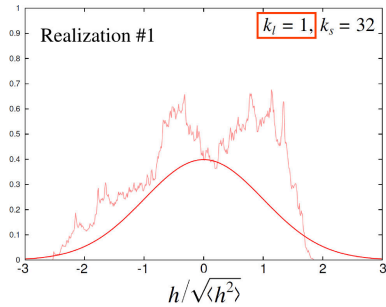
Effect of parameters:

- k_l low frequency cutoff
 - *representativity/normality*^[1,2,3]
- k_s high frequency cutoff
 - *smoothness and density of asperities*
- $\zeta = k_s/k_l$ ratio^[3]
 - *breadth of the spectrum*

$$\alpha \sim \zeta^{2H}$$

Nayak's parameter α is the central characteristic of roughness in asperity based mechanical models.

- [1] Vallet, Lasseux, Sainsot, Zahouani, Tribol. Int. (2009)
- [2] Yastrebov, Durand, Proudhon, Cailletaud, C.R. Mécan. (2011)
- [3] Yastrebov, Anciaux, Molinari, Phys. Rev. E (2012)
- [4] Yastrebov, Anciaux, Molinari, Int. J. Solids Struct. (2015)



Effect of parameters

Effect of parameters:

- k_l low frequency cutoff
 - *representativity/normality*^[1,2,3]
- k_s high frequency cutoff
 - *smoothness and density of asperities*
- $\zeta = k_s/k_l$ ratio^[3]
 - *breadth of the spectrum*

$$\alpha \sim \zeta^{2H}$$

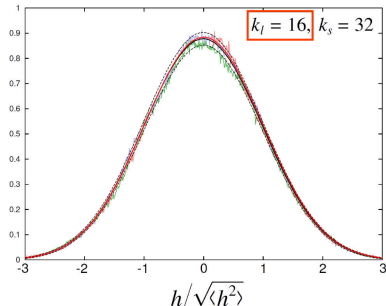
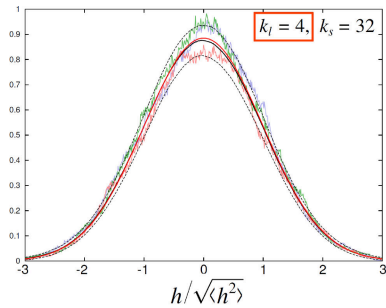
Nayak's parameter α is the central characteristic of roughness in asperity based mechanical models.

[1] Vallet, Lasseux, Sainsot, Zahouani, Tribol. Int. (2009)

[2] Yastrebov, Durand, Proudhon, Cailletaud, C.R. Mécan. (2011)

[3] Yastrebov, Anciaux, Molinari, Phys. Rev. E (2012)

[4] Yastrebov, Anciaux, Molinari, Int. J. Solids Struct. (2015)



Interconnection of parameters

- Spectral moment and k_l, k_s, H :

$$m_{0p} \approx m_{p0} \approx \Phi_0 \int_{k_l}^{k_s} \int_0^{2\pi} [k \cos(\varphi)]^p (k/k_l)^{-2(1+H)} k dk d\varphi = \Phi_0 k_l^{p+2} \frac{\zeta^{p-2H} - 1}{p - 2H} T(p)$$

$$\text{with } T(p) = \int_0^{2\pi} \cos^p(\varphi) d\varphi = \begin{cases} 2\pi, & \text{if } p = 0; \\ \pi, & \text{if } p = 2; \\ 3\pi/4, & \text{if } p = 4. \end{cases}$$

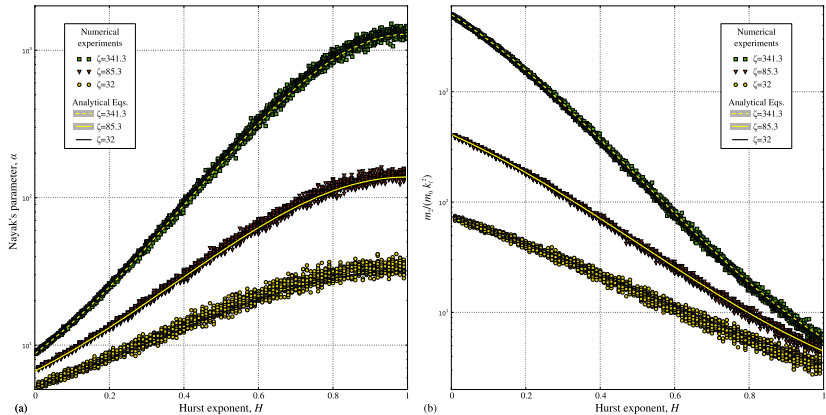
- Nayak's parameter

$$\alpha(H, \zeta) = \frac{3}{2} \frac{(1-H)^2}{H(H-2)} \frac{(\zeta^{-2H} - 1)(\zeta^{4-2H} - 1)}{(\zeta^{2-2H} - 1)^2}$$

- Asperity density

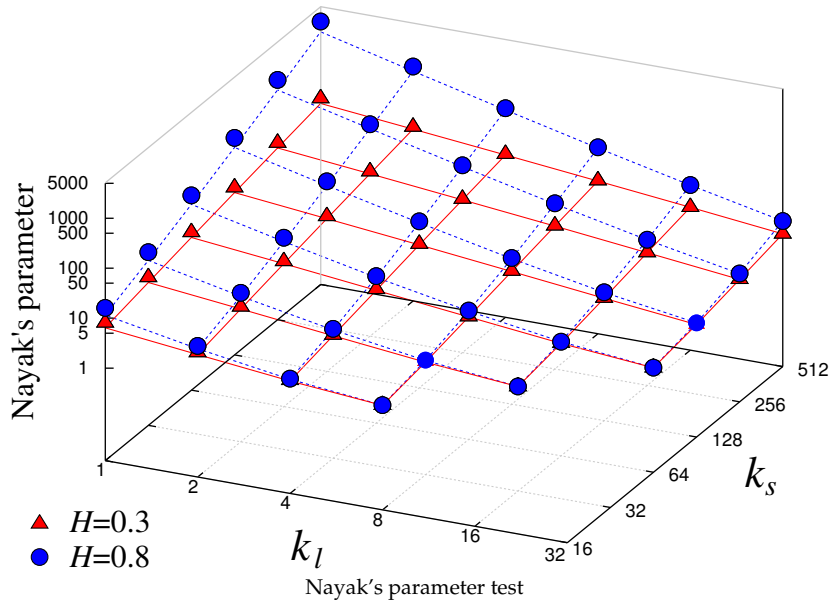
$$D = \frac{\sqrt{3}}{18\pi} \frac{m_4}{m_2} = \frac{\sqrt{3}}{24\pi} \frac{1-H}{2-H} \frac{\zeta^{4-2H} - 1}{\zeta^{2-2H} - 1} k_l^2$$

Interconnection of parameters

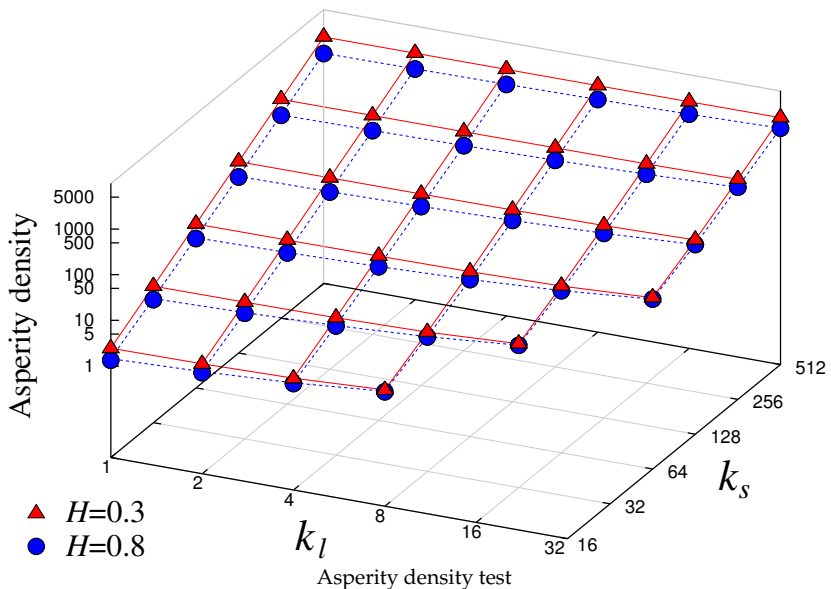


Numerical verification on 100 000 generated rough surfaces with 2048×2048 points

Interconnection of parameters



Interconnection of parameters



Asperity analysis

- Detect summits (z_{ij} higher than neighbouring points) and evaluate second derivatives

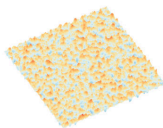
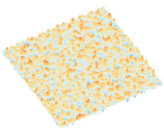
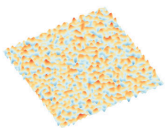
$$\frac{\partial^2 z}{\partial x^2} = \frac{z_{i+1j} + z_{i-1j} - 2z_{ij}}{2\Delta x^2}; \quad \frac{\partial^2 z}{\partial y^2} = \frac{z_{i+1j} + z_{i-1j} - 2z_{ij}}{2\Delta x^2}$$
$$\frac{\partial^2 z}{\partial x \partial y} = \frac{z_{i+1j+1} + z_{i+1j+1} - z_{i+1j-1} - z_{i-1j+1}}{4\Delta x^2}$$

- Principal curvatures $\kappa_{1,2}$:

$$\kappa_{1,2} = \frac{1}{2} \left(\frac{\partial^2 z}{\partial x^2} + \frac{\partial^2 z}{\partial y^2} \right) \pm \sqrt{\left(\frac{\partial^2 z}{\partial x \partial y} \right)^2 + \frac{1}{4} \left(\frac{\partial^2 z}{\partial x^2} - \frac{\partial^2 z}{\partial y^2} \right)^2}$$

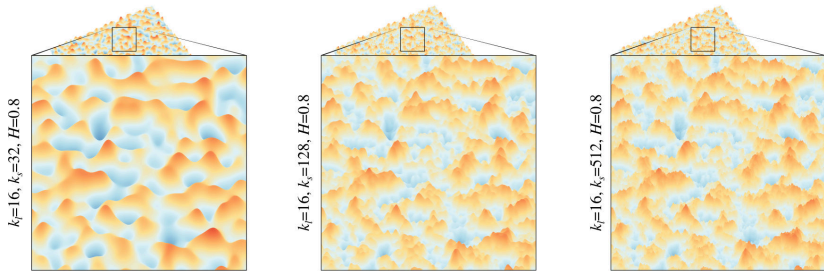
- Saddle point $\kappa_1 \kappa_2 < 0$, extrema $\kappa_1 \kappa_2 > 0$
- Mean curvature which can be safely used in Hertz theory: $\bar{\kappa} = \sqrt{\kappa_1 \kappa_2}$

Asperity analysis



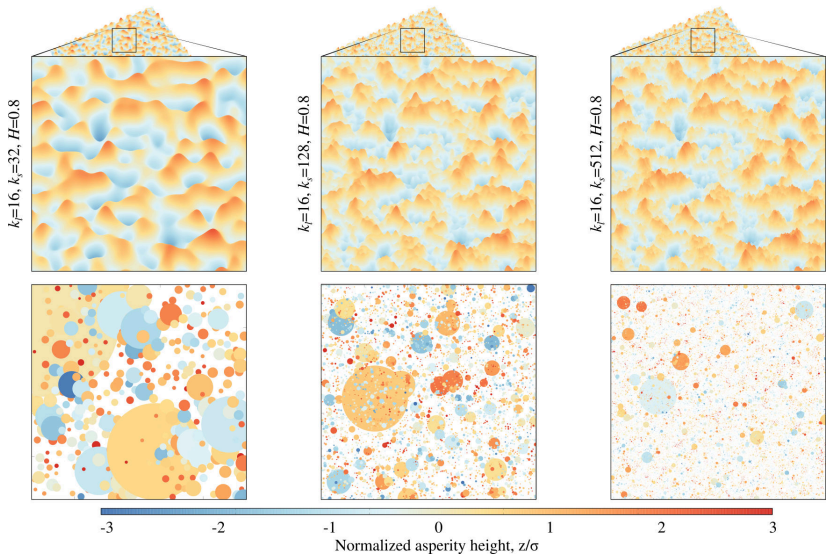
Rough surfaces and associated asperities

Asperity analysis

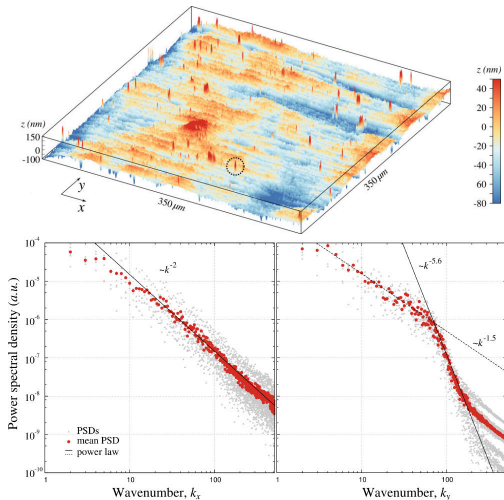


Rough surfaces and associated asperities

Asperity analysis

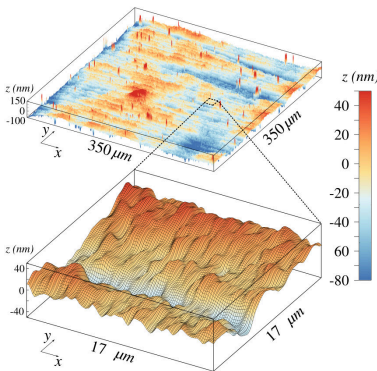


Examples

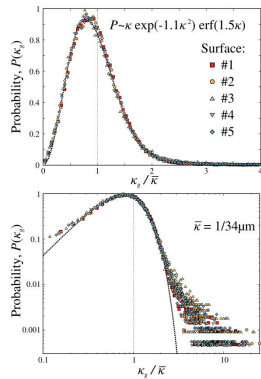


[1] Yastrebov et al, Three-level multi-scale modeling of electrical contacts sensitivity study and experimental validation, Proceedings of Holm Conference, 2015.

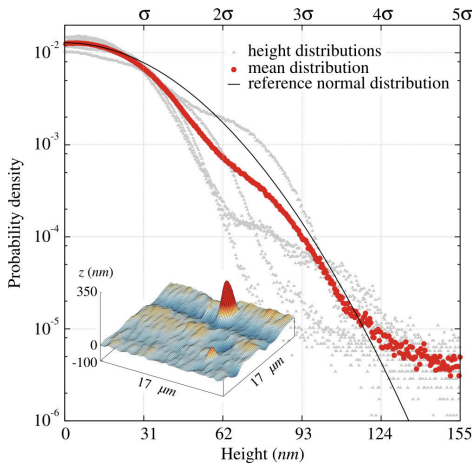
Examples



Asperity curvatures



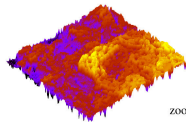
Examples



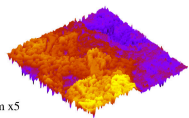
[1] Yastrebov et al, Three-level multi-scale modeling of electrical contacts sensitivity study and experimental validation, Proceedings of Holm Conference, 2015.

Examples

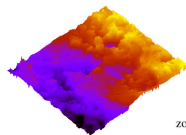
Bright fracture surface



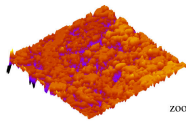
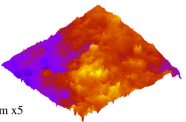
zoom x5



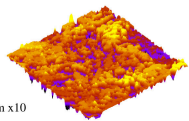
Dark fracture surface



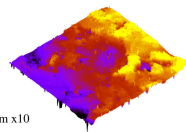
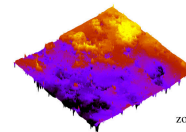
zoom x5



zoom x10

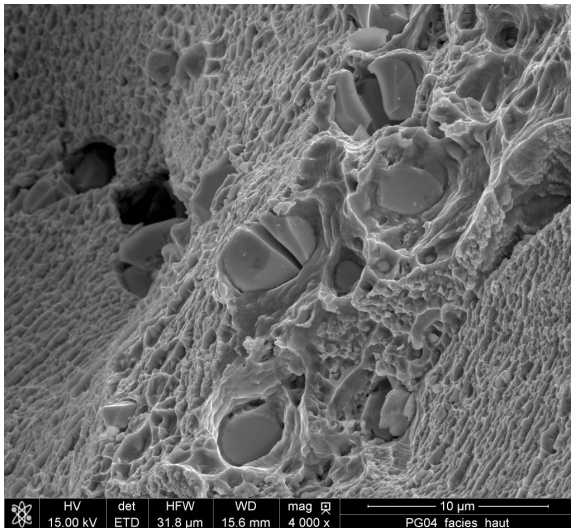


zoom x10



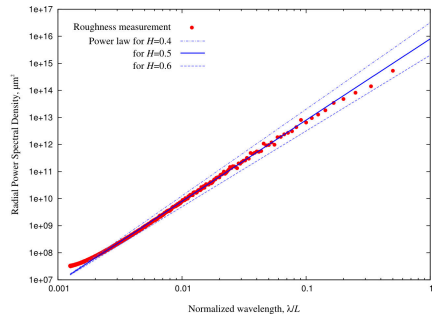
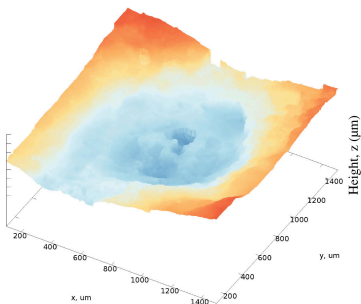
Fatigue & creep fracture surfaces (Ti-alloy)
in collaboration with A. Marchenko

Examples



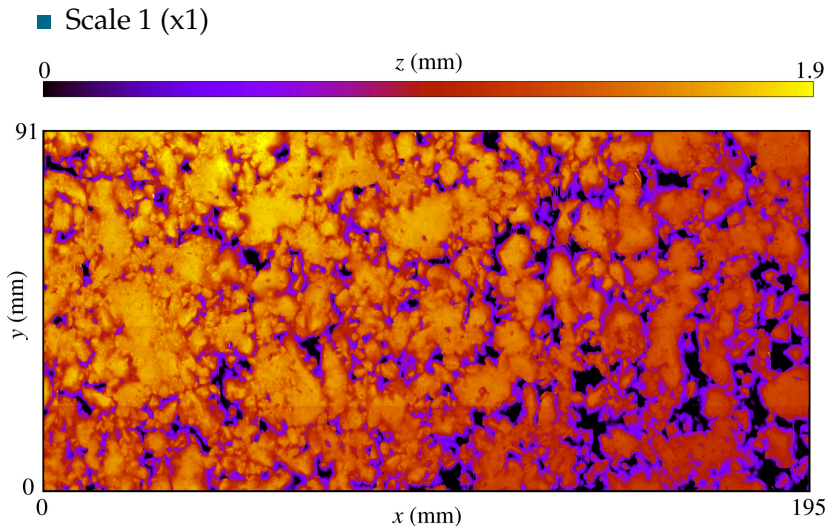
Fatigue fracture surface (Co-alloy), particles WC
Courtesy of V. Esin

Examples

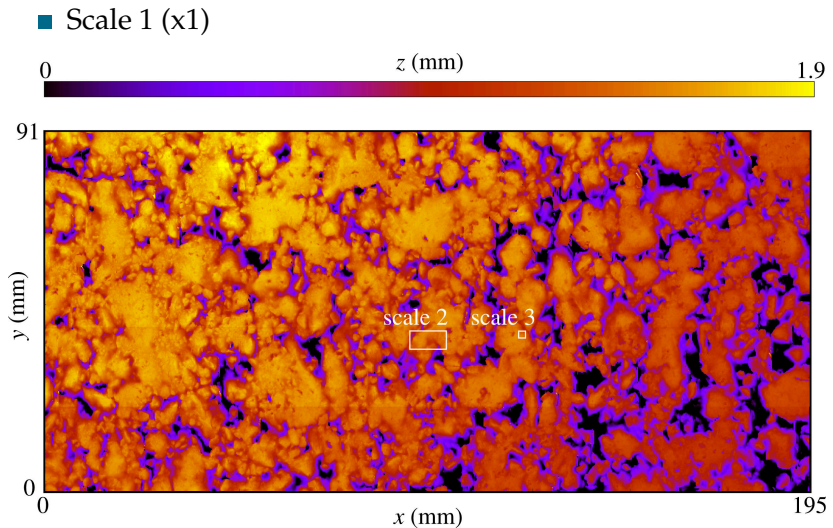


Crater topography and PSD
In collaboration with D. Tkalich (NTNU, Sintef)

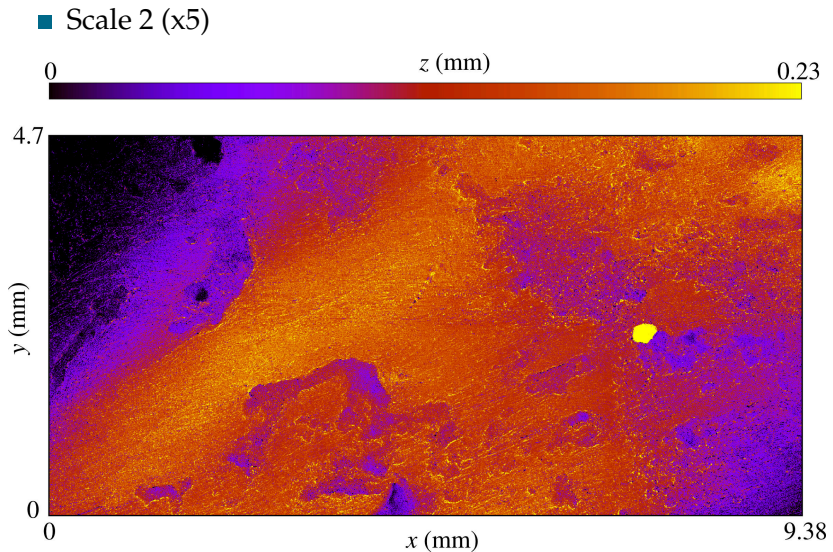
Multiscale road roughness



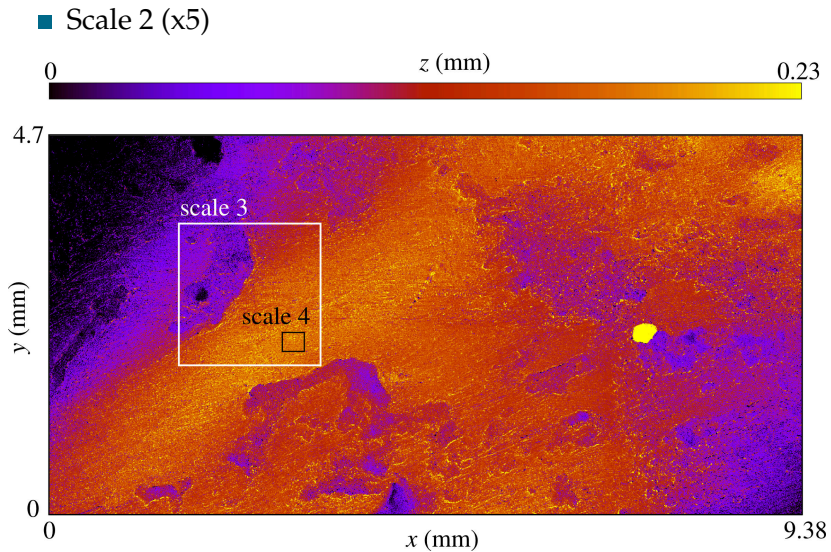
Multiscale road roughness



Multiscale road roughness



Multiscale road roughness



Multiscale road roughness

■ Scale 3 (x20)

0

z (μm)

170.

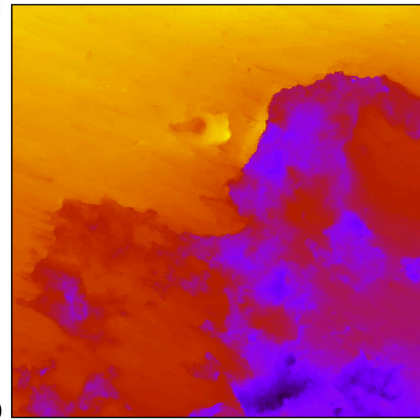
1.76

y (mm)

0

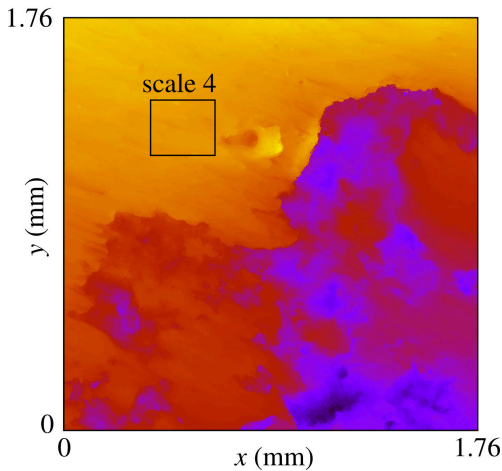
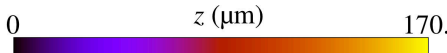
x (mm)

1.76



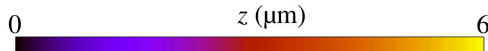
Multiscale road roughness

■ Scale 3 (x20)



Multiscale road roughness

■ Scale 4 (x100)



0.236

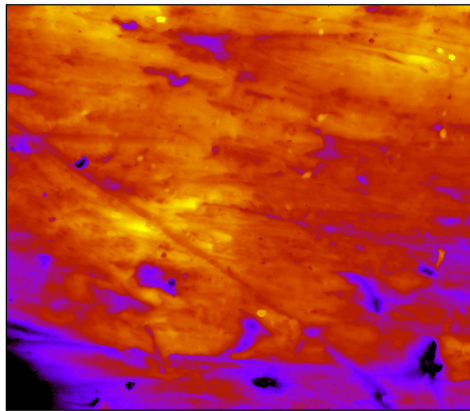
y (mm)

0

0

x (mm)

0.274





Thank you for your attention!
